

**STUDIES ON THERMODYNAMICS AND
QUASINORMAL MODES OF
HIGHER DIMENSIONAL BLACK HOLES**

Thesis submitted to

Cochin University of Science and Technology

in partial fulfillment of the requirements
for the award of the degree of

DOCTOR OF PHILOSOPHY

by

Prasobh C.B.

Theory Division

Department of Physics

Cochin University of Science and Technology

Kochi - 682022

October 2017

*Studies on Thermodynamics and Quasinormal Modes of
Higher Dimensional Black Holes*

PhD thesis in the field of Black Hole Physics

Author

Prasobh C.B.

Department of Physics

Cochin University of Science and Technology

Kochi - 22

mail.prasobhcb@gmail.com

Research Supervisor

Prof V. C. Kuriakose

Department of Physics

Cochin University of Science and Technology

Kochi - 22

vck@cusat.ac.in

this page has been intentionally left blank

CERTIFICATE

Certified that the work presented in this thesis is a bona fide research work done by Mr. Prasobh C.B. under our guidance in the Department of Physics, Cochin University of Science and Technology, Kochi- 682022, India, and has not been included in any other thesis submitted previously for the award of any degree. All the relevant corrections and modifications suggested by the audience during the pre-synopsis seminar and recommended by the Doctoral Committee of the candidate have been incorporated in the thesis.

Kochi-22
October, 2017

Prof. V. C. Kuriakose
(Supervising Guide)

Prof. Ramesh Babu T.
(Joint Guide)

DECLARATION

I hereby declare that the work presented in this thesis is the outcome of the original research work done by me under the guidance of Prof. V. C. Kuriakose and Prof. Ramesh Babu T., Department of Physics, Cochin University of Science and Technology, Kochi-682022, India, and that it is not part of any other dissertation submitted for the award of any degree, diploma, associateship, or any other title or recognition from any University or institution.

Kochi-22
October, 2017

Prasobh C.B.

Contents

Table of Contents	ix
Preface	xi
List of Publications	xv
Acknowledgements	xvi
1 Introduction	1
1.1 Relevance of Higher Dimensional Black Hole Physics	1
1.2 Higher Dimensional Models of Gravity - The Lovelock Model	6
1.3 Quasinormal Modes of Black Holes and their Asymptotic Forms	11
1.4 AdS - CFT Correspondence and QNMs	16
1.5 QNMs, Asymptotic QNMs and Gravitational Radiation in Higher Dimensions	19
1.6 Black Hole Thermodynamics and Black Hole Geometrother- modynamics	21
1.7 Black Hole Thermodynamic Geometry	26
1.8 Structure of the Thesis	29
2 Scalar Field Evolution and Area Spectrum for Lovelock- AdS Black Holes	33
2.1 Introduction	33
2.2 The Metric and the Numerical Computation of Quasinor- mal Frequencies	38
2.3 Discussion on Results of the Numerical Calculation	44
2.4 Asymptotic Quasinormal Modes and Area Spectrum of Large Black Holes	46
2.4.1 Area Spectrum	53
2.5 Conclusion	55
3 Quasinormal Modes of Lovelock Black Holes	57
3.1 Introduction	57
3.2 Geodesic Stability	60
3.2.1 The Equations of Perturbation and the WKB Method	61

3.2.2	Asymptotic Quasinormal Modes in terms of Null Geodesic Parameters	65
3.3	Results and Discussion	67
3.4	Conclusion	83
4	Thermodynamics of Charged Lovelock - AdS Black Holes	85
4.1	Introduction	85
4.2	Thermodynamic Stability of Charged AdS Black Holes in Lovelock Model	89
4.3	Geometrothermodynamic (GTD) Analysis	100
4.4	Area Spectrum of Large Charged AdS Black Holes in Lovelock Model	104
4.5	Conclusions	107
5	Summary	111
5.1	Prospects of Future Work	114
	References	117

Preface

The idea that the dimensionality of the spacetime describing the Universe may be different from four is almost as old as the General Theory of Relativity (GTR) itself, originating in the early twentieth century, when Kaluza and Klein succeeded for the first time in combining the theories of electromagnetism and gravity into a single unified theory that would only make sense in a five dimensional spacetime. It is currently known that the unification of fundamental forces in nature involves higher dimensional spacetimes. During the decades that followed, quantum leaps in technology increased mankind's grasp on the forces of nature manifold. We now know that there are four fundamental forces in nature, two of which were completely unknown during Einstein's time, which must have been one of the reasons why his attempts at complete unification were ultimately unfruitful. Unfortunately, we are yet to succeed completely where he failed, and a unified theory of forces, in a fully consistent and satisfactory form, still isn't available. The best candidates to date, in the opinions of the majority, are the string theory and M-theory, both of which make sense only in higher dimensional spacetimes. This is one of the reasons why study of gravity in higher dimensions is of considerable relevance. Another reason would be the expected creation of higher dimensional mini black holes inside particle accelerators such as the LHC when TeV scale energies are reached. Add to these the fact that many equations governing the evolution of physical fields contain dimension-dependent terms. Some of these terms identically vanish in four dimensions. One would be interested to know about the consequence of the presence of these terms on the physics in the vicinity of black holes. In addition to all these practical considerations, it is of immense intrinsic theoretical interest to study higher dimensional gravity, the mathematical insights gained from which

could prove useful in other areas.

The parallels between black hole physics and thermodynamics, conjectured first by Bekenstein and based on insight on processes like the quantum radiation from event horizons, actually extends much beyond a simple similarity between equations of black hole dynamics and the laws of thermodynamics. Black hole event horizons are treated on the same footing as thermodynamic systems in literature and attributed with thermodynamic parameters like temperature, entropy, specific heat, etc...Study of the thermodynamic properties of black hole event horizons is expected to shed light on the microscopic structure of spacetime. Transition between different stable phases of black hole spacetimes is also an active area of research and is often carried out by studying the specific heat of event horizons. Methods of differential geometry can also be used in conjunction with the ordinary methods to study such phase transitions.

When we probe gravity in higher dimensions, however, limitations of the General Theory of Relativity, which is the most satisfactory theory in four dimensions, become apparent. Hence the need to find more general theories of gravity. Of the various methods using which GTR could be generalized, the most obvious one is to add terms to the Lagrangian of the theory terms that are of higher-than-one order in the curvature tensor and the corresponding curvature scalar. Corresponding to Lagrangians that are quadratic, cubic etc. in the curvature, we have second, third, etc. order theories of gravity. Of such theories, the Lovelock model of gravity is considered to be the natural generalization of GTR to higher dimensions, yields field equations that are of second order in the metric tensor and forms the basis

of the works presented in this thesis. The thesis details studies on the dynamics of fields in, and thermodynamics of, maximally symmetric solutions to the Lovelock model having a unique cosmological constant at all orders and dimensions. Dynamics of fields is studied in terms of the quasinormal frequencies of perturbations to the background spacetimes and thermodynamics of the black hole spacetimes is studied using two methods—the usual method of calculating the specific heat of the black hole event horizon and using methods of differential geometry. The latter serves as a tool for corroborating the deductions from the former. We attempt to perform these studies taking the spacetime dimension d and the order of the theory k as parameters.

The thesis consists of five chapters.

Chapter 1 touches upon the motivations behind conducting research on black hole physics in higher dimensions. Different motivating factors, including the AdS-CFT correspondence between theories of gravity and Quantum Field Theory, are discussed, emphasizing on how studies performed in one area could help further our insight in the other. It also contains a brief review on the research already performed in the area and introduces concepts like the Quasinormal modes of perturbations and their asymptotic forms, including their practical utility in light of the AdS-CFT correspondence. A brief section on the structure of the Lovelock model of gravity also forms part of this chapter.

In **Chapter 2**, we study the dynamics of scalar fields in maximally symmetric, asymptotically AdS black hole spacetimes in Love-

lock model. This is done by calculating the quasinormal frequencies of the field equation using the Horowitz-Hubeny numerical method. The calculation is done for different spacetime dimensions and for different values of the order k of the model. We also calculate the asymptotic form of these QNFs analytically and deduce the form of the area spectrum of the event horizon from the asymptotic form.

Chapter 3 contains the details of the calculation of quasinormal frequencies of scalar, vector and tensor perturbations in asymptotically flat, maximally symmetric black hole spacetimes in the Lovelock model. The numerical calculation is performed using the sixth order WKB method. The form of the quasinormal frequencies for very large values of the mode number l is analytically found. The numerical results and the analytical expression are used in order to study how the quasinormal frequency varies as the spacetime dimension d and the order of the theory k vary.

We investigate the thermodynamics of charged black holes in asymptotically AdS spacetimes in **Chapter 4**. Thermodynamic parameters of the black holes like the horizon temperature, entropy, etc... are calculated in terms of the horizon radius, which is taken as the control parameter. Phase transitions in the spacetime are investigated by calculating the specific heat of the event horizon and finding out the points of divergence. The methods of black hole geometrothermodynamics are used to calculate the thermodynamic curvature of the spacetime and find out the points of divergence, signifying such phase transitions.

Chapter 5 summarizes the main conclusions drawn from the studies described in this thesis. It also mentions prospects of work that could be done on the topics that are studied.

Part of this work have been published as papers in refereed journals. Details are given below:

Publications in refereed journals

1. C.B. Prasobh and V.C. Kuriakose, *Scalar field evolution and area spectrum for Lovelock-AdS black holes*, **Gen. Relativ. Gravit.** (2013) **45:2441–2456**
2. C.B. Prasobh and V.C. Kuriakose, *Quasinormal modes of Lovelock black holes*, **Eur. Phys. J. C** (2014) **74:3136**
3. C.B. Prasobh, Jishnu Suresh and V.C. Kuriakose, *Thermodynamics of charged AdS-Lovelock black holes*, **Eur. Phys. J. C** (2016) **76:207**

Acknowledgements

First and foremost, I salute GOD the Almighty...

I would like to express my sincere and heartfelt gratitude to my guide, Dr. V. C. Kuriakose, Dept. of Physics, CUSAT, for the boundless support and guidance - both academic and personal - that he has provided throughout the years and the infinite patience that he showed, especially towards the end of my stint at the department as a part - time student. His deep knowledge, constant encouragement and truthful criticism are the reasons for whatever little progress that was made during these years.

I also thank my co-guide, Dr. Ramesh Babu T., Dept. of Physics, CUSAT, for his enthusiastic support for my research throughout the years.

I would also like to extend my sincere thanks to the present Prof. and Head of the Department, Dr. Junaid Bushiri and former HODs, for providing the necessary facilities and administrative support for my research throughout the years. The same goes for all the current and former teaching, non - teaching and library staff of the Dept. of Physics as well as the current and former Administrative staff of CUSAT.

I would like to acknowledge the support extended to my research by IUCAA in the form of computational facilities provided at the IUCAA Resource Center. I also acknowledge financial support from CSIR, New Delhi, in the form of JRF under CSIR Emeritus Scien-

tistship Scheme awarded to my guide and UGC, New Delhi, under the RFSMS.

The years that I spent at the Dept. were memorable mainly due to the association that I have had the good fortune to enjoy with the research scholars there, especially those in the theory division. I have many fond memories of the discussions and chats that I had with my fellow scholars - Nijo, Tharanath, Saneesh, Jishnu, Lini, Vivek, Prasia, to name just a few who worked under the same guide as that of mine. Of these, all but Jishnu and Prasia are my seniors and helped me a great deal especially during the early years of research. Prasia and Jishnu joined later and Jishnu became the co-author of one of my papers. He and Lini were my eyes, ears and hands at the Department after I became a part - time student in 2014. Conversations with Jishnu, especially on theoretical subjects, helped me gain further insight into the subjects and to ease the pressure to get published, when the conversations were about other topics, such as travel, video games, etc. Lini, who was my senior during my undergraduate and postgraduate years as well, went through a lot of trouble for me, especially during the past few months, be it for remitting the semester fee on my behalf or for procuring necessary administrative documents. I will always remember these with warmth and gratitude. Anoop, Priyesh and Shaju Sir worked under Ramesh Sir for almost the entire period during which I was a full - time research student, and I have warm memories of the close friendship that I had with them. Jerin joined the Department under Titus Sir after I became a part - time student, always ready to extend a helping hand whenever I need someone to get something done at CUSAT. I express my heartfelt gratitude to all of these people.

My parents, my brother and my sister - in - law constitute my immediate family along with Sambhu and Vavaji - my nephews. They are the reason for whatever I am today. Whatever little I have achieved in my life, they are the reason. Sambhu and Vavaji - both of them - were born after my PG and grew up during my research. Spend a few seconds with either of them and I find it astounding that all troubles - academic or personal - can melt away so quickly.

*All of this - the support and encouragement of all of these people - would've been for nought, had another person not been there for me - this thesis wouldn't have taken form without that person. Without naming, let me address that person - **you** know who you are ... without you, this - the submission of this thesis - wouldn't have happened ... all would've been lost between the cup and the lips...*

Prasobh C.B.

1

Introduction

1.1 Relevance of Higher Dimensional Black Hole Physics

The interest in pursuing theories of gravity in higher dimensional spacetimes can be justified on multiple fronts - there is the obvious and intrinsic theoretical curiosity about the structure of higher dimensional spacetimes and properties of physical fields in such spacetimes. This is adequately articulated by a pioneer in the field of higher dimensional gravity, F.R. Tangherlini, the one who generalized Einstein - Hilbert gravity to an asymptotically flat n dimensional spacetime and derived the metric representing the same [27]. To quote,

“...[The fact that mathematical expressions describing the laws of nature exhibit a greater generality regarding the dimensionality of spacetime than space itself exhibits on a macroscopic scale] is readily seen upon examination of Newton’s laws of motion, the Lagrangian and Hamiltonian formalisms, the two principles underlying special relativity, the principle of equivalence, the principle of general covariance, the geodesic principle, and the principles of quantum mechanics. In none of the above - cited cases do either the statements of the principles or the mathematical machinery restrict us to three dimensions...”

Black holes, as we know them today, are regions of spacetime where the curvature of the spacetime is so large that every kind of signal emitted from the region or entering the region would get infinitely red shifted so as to make “observation” of the “interior” of the region impossible. In simpler terms, not even light can escape the region, as the well - known definition says. These black holes are always accompanied, at least in four dimensions, by what is called an event horizon, which is a subspace of the original spacetime, acting as the de - facto boundary of the region.

According to a conjecture known as the no - hair theorem, black holes in four dimensional spacetimes are characterized by three of parameters - mass, charge and angular momentum. They also obey a number of laws such as ones similar to the laws of ordinary thermodynamics. Also, there exists a number of constraints on how black holes can exist, and the number of parameters that can specify the end state of evolution of a black hole, etc. - Birkhoff’s theorem, Cosmic censorship conjecture etc. are a few among them. It would be of interest to know if such laws can be extended to the case of black holes in higher dimensions, or if they are unique to four dimensions. Related to this are the questions regarding the stability - both the stability against perturbations and thermodynamic stability - of black holes. Do black holes that are stable against perturbations at four dimensions become unstable at higher dimensions? Do the important thermodynamic quantities related to black holes - such as the specific heat of their event horizons - depend on the dimensionality of the spacetime? Does the dimensionality of the spacetime play a role in determining their thermodynamic stability?

In addition to such intrinsic curiosity, there are other motivations as well for studying black holes in higher dimensions. One of these comes from attempts to unify the four fundamental forces of nature. The most important candidates for the status of such “Theory of Everything” are the string theory and M - theory, both of which can be consistently defined only in higher dimensional spacetimes. It is known that, at low energies, these theories reduce to supergravity theories. What makes these interesting is the fact that solutions of these theories that admit the existence of event horizons - called black objects - help explain the quantum mechanical origins of black hole entropy among other physical properties [67–69].

Yet another motivation for considering black hole physics in higher dimensional theories comes from the so - called gauge - gravity correspondence [3], which is the observation that there exists a dual relation between theories of gravity defined in an n dimensional, asymptotically AdS spacetime and a strongly coupled gauge theory in $n - 1$ dimensions. The gauge - gravity correspondence makes it possible to compute physical parameters of a strongly coupled system by studying the corresponding gravitational system in the next higher dimension. Hence the interest in gravity in higher dimensional, asymptotically AdS spacetimes.

Another feature of higher dimensional black hole physics that warrants attention is the existence of critical dimensions [83]. In many higher dimensional black hole solutions of theories of gravity, there exist multi - phase spacetimes. What it means is that the horizon topology can change as a function of certain parameters related to the spacetime. It is known that there exist changes between such

phases of black objects. A famous example of such black hole phase change, known as the Gregory - Laflamme (GL) instability [22], has dependence on the spacetime dimensions.

Simply put, the GL instability involves the splitting up of a uniform black string into a non - uniform black string, which could lead to the formation of several black holes along the length of the string. The transition takes place at what is called the Gregory - Laflamme point, which is where the instability sets in. The interesting property, and what makes the GL instability relevant within the context of higher dimensional gravity, is the existence of a critical dimension at which the transition between the black string and the black hole phases changes from first order to second order.

The GL instability is not the only kind of instability that the black hole solutions suffer from. It is known in the literature that dynamic stability of black holes - that is, stability of the evolution of physical fields in the spacetime - is also dependent on the dimension of the spacetime. The stability of black hole spacetimes against perturbations is decided by various factors including the asymptotic behavior and dimensionality of the spacetime, the symmetries of the tangent space, etc. The uniqueness theorem which applies to the final state of the gravitational collapse of matter with static and spherically symmetric initial conditions, also known as Birkhoff's theorem, breaks down in higher dimensions [4]. Consequently, the boundary conditions for perturbations also change. The uniqueness and the spherical symmetry of the horizon geometry in four dimensions is mainly responsible for the stability exhibited by the solutions of General Theory of Relativity(GTR) against various perturbations. They do not

hold in higher dimensions [4] with permissible solutions having $S^2 \times S^1$ topology called Black Rings. However, in the static asymptotically flat case [27], such a violation has not been proved yet. Once the condition of asymptotic flatness is dropped, this uniqueness fails and there exist an infinite number of discrete solutions [5]. In n dimensions, these solutions are obtained by replacing the metric on the spherical $(n - 2)$ dimensional subspace with any other Einstein manifold whose Ricci curvature has the same magnitude as that of a unit round $(n - 2)$ sphere. Bohm metrics [6] belong to this class and have been proved [7] to represent spaces with lower volume compared to S^{n-2} . The stability of perturbations in such spacetimes is related to the spectrum of the Lichnerowicz operator on the tangent space [8] which depends on the dimension of the spacetime.

Stability of generalized black hole solutions against tensor perturbations in AdS spacetimes has been discussed by Hartnoll [9]. It has been found that the lower bound of the spectrum of the Lichnerowicz operator, and in turn the stability, depends on the size of the black hole as well as the dimension in AdS spacetimes. In the case of very large black holes, the analysis shows that there exists a suitable Bohm metric with eigenvalues that are sufficiently negative so as to destabilize the spacetime. Interestingly, these large black hole solutions are locally thermodynamically stable. As the size of the black hole is increased, the critical eigenvalue becomes increasingly negative. For small black holes, it is found that the criterion for stability in the asymptotically flat case is recovered.

The facts listed in the preceding paragraphs clearly explain the importance of studying black hole physics in higher dimensional space-

times. However, when we go to higher dimensions, we see that the original theory of gravity, namely the General Theory of Relativity (GTR), is no longer the most general theory of gravity. Hence the need to consider more generalized models of gravity.

1.2 Higher Dimensional Models of Gravity - The Lovelock Model

There are practical reasons for considering more generalized theories in both four and higher dimensions. One such reason is the failure of GTR to explain phenomena like the late - time accelerated expansion of the universe [149]. GTR is also inadequate to explain the origin and properties of dark matter and dark energy. Though various attempts have been made to find an alternative theory to GTR in order to explain such astronomical observations and to overcome the conceptual difficulties encountered in GTR, we have yet to arrive at a successful theory. Even though there are attempts at explaining the expansion based on the cosmological constant, known in the literature as the Λ CDM model, it is not without its problems, such as the coincidence problem, the discrepancy in the observed magnitude of the cosmological constant, etc. Attempts at explaining the dark energy problem in terms of ad - hoc scalar fields, known as quintessence, are also known. However, when we study gravity in higher spacetime dimensions, we realize that it is not enough to focus our attention on corrections to first order theories like GTR, since GTR is not the most general theory of gravity in such spacetimes - we must also consider the possibility of generalizing GTR without introducing such fields. Such attempts could focus on modifying the action that GTR is based on. GTR is derived, as is well known, from a Lagrangian

Higher Dimensional Models of Gravity - The Lovelock Model⁷

which is linear in the Ricci curvature scalar. One way, therefore, of generalizing it, would be to add terms to it that are of higher - than - one degree in the curvature scalar. In this respect, a set of theories of gravity, known as the $f(R)$ model, are relevant. They are capable of explaining observations like the expansion of the universe, the rotation - curves of galaxies, etc. One issue that one encounters, however, with the $f(R)$ model, is that the action in that model produces field equations that are of order four in the components of the metric tensor. It is cumbersome to analyze the behavior of physical systems in a background spacetime described by a fourth order equation.

We, therefore, seek a model of gravity that is derived from a Lagrangian that contains higher order curvature terms while, at the same time, yields field equations that are of second order in the metric tensor, just like the case of GTR. The Lanczos - Lovelock model of gravity [40, 41, 145] is based on the most general Lagrangian based on the same principle as that of GTR, namely general covariance, and hence considered to be the natural generalization of GTR to higher dimensions [50]. The studies that have been carried out in this thesis are all based on solutions of this model. The following paragraphs explain the mathematical structure of the Lovelock Lagrangian and the form of the static and spherically symmetric solutions that it admits.

The Lovelock Lagrangian contains dimensionally extended Euler characteristic densities [14] which contain higher powers of the Riemann curvature tensor than one. The most general symmetric, divergence free and ghost free (ie. with no negative norm eigenstate in the corresponding quantized theory) rank (1,1) tensor, which can be constructed out of the metric and its first and second derivatives,

analogous to the Einstein tensor in GTR, is constructed out of this Lagrangian. The Lovelock Lagrangian in a D dimensional spacetime is written in the form

$$L = \sum_{m=0}^k c_m \mathcal{L}_m , \quad (1.1)$$

where $k \equiv \lfloor \frac{D-1}{2} \rfloor$ which is the integer part of $\frac{D-1}{2}$. \mathcal{L}_m , defined as

$$\mathcal{L}_m \equiv \frac{1}{2^m} \delta_{\rho_1 \kappa_1 \dots \rho_m \kappa_m}^{\lambda_1 \sigma_1 \dots \lambda_m \sigma_m} R_{\lambda_1 \sigma_1}^{\rho_1 \kappa_1} \dots R_{\lambda_m \sigma_m}^{\rho_m \kappa_m} , \quad (1.2)$$

is the m^{th} order dimensionally extended Lovelock term. $R_{\lambda\sigma}^{\rho\kappa}$ is the Riemann tensor in D - dimensions and $\delta_{\rho_1 \kappa_1 \dots \rho_m \kappa_m}^{\lambda_1 \sigma_1 \dots \lambda_m \sigma_m}$ is the generalized Kronecker delta. The Lovelock term with $2m = D$ becomes a total divergence and those with $2m > D$ vanish [145]. Therefore the maximum order of terms in L is determined by the dimension of the spacetime. c_m are constants. We set $c_0 = -2\Lambda$, $c_1 = 1$ and $c_m = a_m/m$ ($m \geq 2$). The field equations in Lovelock model, derived by varying the action w.r.t. the metric are given by,

$$0 = \mathcal{G}_\mu^\nu = \Lambda \delta_\mu^\nu - \sum_{m=1}^k \frac{1}{2^{(m+1)}} \frac{a_m}{m} \delta_{\mu \rho_1 \kappa_1 \dots \rho_m \kappa_m}^{\nu \lambda_1 \sigma_1 \dots \lambda_m \sigma_m} R_{\lambda_1 \sigma_1}^{\rho_1 \kappa_1} \dots R_{\lambda_m \sigma_m}^{\rho_m \kappa_m} , \quad (1.3)$$

where \mathcal{G}_μ^ν , called the Lovelock tensor [56] is the generalization of the Einstein tensor to higher orders. We write the static and spherically symmetric solutions to the Lovelock equations as,

$$ds^2 = -f(r)dt^2 + \frac{dr^2}{f(r)} + r^2 \gamma_{ij} dx^i dx^j , \quad (1.4)$$

where γ_{ij} is the metric on the ($n \equiv D - 2$) dimensional constant curvature tangent space with a curvature $\kappa=1$. Specifically we take the form of γ_{ij} as [14],

$$\gamma_{ij} = \delta_{ij} + \frac{x_i x_j}{1 - x^2} . \quad (1.5)$$

Using this metric ansatz, we compute the components of the Riemann curvature tensor as,

$$R_{tr}^{tr} = -\frac{f''}{2}, \quad R_{ti}^{tj} = -\frac{f'}{2r} \delta_i^j = R_{ri}^{rj}, \quad R_{ij}^{kl} = \left(\frac{\kappa - f}{r^2} \right) (\delta_i^k \delta_j^l - \delta_i^l \delta_j^k) . \quad (1.6)$$

We define a new variable $\psi(r)$ by,

$$f(r) = \kappa - r^2 \psi(r) , \quad (1.7)$$

and indicate the angle variables by indices like i, j, k, l etc. We substitute (1.4), (1.5) and (1.6) into (1.3) with $\mu = \nu$ to get

$$\begin{aligned} 0 &= \Lambda - \sum_{m=1}^k \frac{1}{2^{m+1}} \frac{a_m}{m} \left[(2^{m-1}) 2m \delta_{rj_1 \dots j_{2m-1}}^{ri_1 \dots i_{2m-1}} R_{ri}^{rj} (R_{kl}^{pq})^{m-1} + (2^m) \delta_{j_1 \dots j_{2m}}^{i_1 \dots i_{2m}} (R_{kl}^{pq})^m \right] , \\ &= \Lambda - \sum_{m=1}^k \frac{a_m}{m} \left[\left(\frac{1}{4} \right) 2m \delta_{j_1 \dots j_{2m-1}}^{i_1 \dots i_{2m-1}} \left(-\frac{f'}{2r} \right) \delta_{i_1}^{j_1} \psi^{m-1} \delta_{i_2}^{j_2} \dots \delta_{i_{2m-2}}^{j_{2m-2}} \right. \\ &\quad \left. + \left(\frac{1}{2} \right) \delta_{j_1 \dots j_{2m}}^{i_1 \dots i_{2m}} \psi^m \delta_{i_1}^{j_1} \dots \delta_{i_{2m}}^{j_{2m}} \right] . \quad (1.8) \end{aligned}$$

(We have $\delta_{\mu\rho_1\kappa_1 \dots \rho_m\kappa_m}^{\mu\lambda_1\sigma_1 \dots \lambda_m\sigma_m} = \delta_{\rho_1\kappa_1 \dots \rho_m\kappa_m}^{\lambda_1\sigma_1 \dots \lambda_m\sigma_m}$ since $\delta_{\mu}^{\nu} = 0$ when $\mu \neq \nu$. We split the general term of order m in (1.3) in to two - those with m factors of the form R_{ij}^{kl} and those with one factor of the form R_{ti}^{tj} or R_{ri}^{rj} and $(m-1)$ factors like R_{ij}^{kl} . There are m terms each of the latter type and each factor like R_{ij}^{kl} has to be multiplied by 2. Also, $R_{ti}^{tj} = R_{ri}^{rj}$. Observing these facts, we substitute the forms of R_{ti}^{tj} , R_{ri}^{rj} and R_{ij}^{kl} into (1.3) in order to get the expression given above.)

We exploit the property of the generalized Kronecker delta, namely

$$\delta_{i_1 \dots i_m}^{j_1 \dots j_m} \delta_{j_1}^{i_1} = \{n - (m - 1)\} \delta_{i_2 \dots i_m}^{j_2 \dots j_m},$$

in order to write (1.8) in the form

$$\begin{aligned} 0 &= \Lambda - \frac{n}{2} \sum_{m=1}^k \frac{a_m}{m} \left\{ \prod_{p=1}^{2m-2} (n-p) \right\} \left[m \frac{(r^2 \psi)'}{r} \psi^{m-1} + (n-2m+1) \psi^m \right], \\ &= \Lambda - \frac{n}{2} \sum_{m=1}^k \frac{a_m}{m} \left\{ \prod_{p=1}^{2m-2} (n-p) \right\} \left[\frac{m (r^2 \psi)^{m-1} (r^2 \psi)'}{r^{2m-1}} \right. \\ &\quad \left. + \frac{(n-2m+1) r^{n-2m} (r^2 \psi)^m}{r^n} \right], \\ \text{i.e. } 0 &= 2\Lambda r^n - n \sum_{m=1}^k \frac{a_m}{m} \left\{ \prod_{p=1}^{2m-2} (n-p) \right\} \left[r^{n+1} \psi^m \right]'. \end{aligned} \quad (1.9)$$

Integrating (1.9) first with respect to r and then over the spherically symmetric tangent space of dimension n , we get a polynomial expression that must be satisfied by the spherically symmetric solutions to the Lovelock model, namely

$$W[\psi] \equiv \sum_{m=2}^k \left[\frac{a_m}{m} \left\{ \prod_{p=1}^{2m-2} (n-p) \right\} \psi^m \right] + \psi - \frac{2\Lambda}{n(n+1)} = \frac{\mu}{r^{n+1}}, \quad (1.10)$$

where μ is a constant of integration related to the black hole mass M as,

$$M = \frac{\mu \pi^{n/2}}{\Gamma\left(\frac{n+1}{2}\right)}. \quad (1.11)$$

1.3 Quasinormal Modes of Black Holes and their Asymptotic Forms

We develop our knowledge of black hole physics by analyzing the dynamics of physical fields in the vicinity of the event horizons of black holes. Presence of physical fields near the horizon would present itself as a perturbation to the background spacetime metric. It is known [32, 33, 150] that such perturbations - whether tensor, vector or scalar in type - evolve in time in different stages, known as initial outburst, quasinormal ringing and power law decay. Of these three, the second phase is the one during which the emission of gravitational waves is supposed to be at a maximum. This phase is supposed to be observable using Gravitational Wave (GW) antennas and dominated by the so - called Quasinormal modes (QNMs), which are modes of the field of perturbation having complex frequency of oscillations. In other words, QNMs represent damped oscillations of the metric perturbations. The corresponding frequencies are called QN frequencies and are important parameters determining the dynamics of the fields.

Mathematically, QNMs, discovered by Vishveshwara [82], are solutions of field equations that govern the evolution of physical fields in spacetimes that contain black holes. As mentioned in the preceding paragraph, the evolution mainly contains three stages - an initial outburst, an oscillatory stage and a late - time decay stage. QNMs characterize the second stage, called the quasinormal ringing phase. the physical field in the vicinity of the black hole can be considered as a perturbation to the background spacetime. Such perturbations can be of various types - gravitational, scalar, vector, spinor, dirac, etc. The frequency of oscillations in the second stage is called the

quasinormal frequency (QNF). The word “quasi” signifies the fact that these frequencies are complex in nature, thus describing damped oscillations. The real part of the QNF would then represent the actual frequency of oscillations and the imaginary part would represent the damping time of the oscillations.

QNMs of perturbations are obtained as solutions of the respective field equations, when solved with respect to the metric that describes the particular black hole spacetime of interest. Such field equations, in the case of static, spherically symmetric spacetimes, take a Schrödinger - like form with an effective potential that depends both on the nature of the perturbing field and on the parameters of the black hole. In the case of asymptotically flat spacetimes, the effective potential that is perceived by the field in the spacetime often resembles a finite potential barrier such that the potential vanishes at infinity. This leads to the possibility of obtaining solutions that are purely ingoing at the event horizon of the black hole and purely outgoing at infinity, both resembling plane waves when expressed in terms of a scaled co - ordinate called the tortoise co - ordinate. The well - known WKB approximation is applicable in such situations and it provides a particularly convenient way of computing the QNFs in these spacetimes [71]. In the case of asymptotically AdS spacetimes, however, the potential grows indefinitely at infinity, due to the presence of the Λ term in the metric. Such a potential, which diverges at spatial infinity, effectively confines the field and provides a situation similar to the “particle - in - a - box” problem in elementary quantum mechanics. Motivated by the method of solution of such problems, we change the boundary conditions that the solutions are supposed to satisfy. Whereas the solutions in the asymptotically flat case are

supposed to be wave - like at the horizon as well as at spatial infinity, in the AdS case, one usually looks for solutions that vanish at infinity, the boundary condition at the event horizon being left unchanged [37].

The significance of QNMs in black hole physics stems from the fact that the QNFs are characteristic of the black hole itself, and not dependent on the nature of the perturbations. What it means is that the values of the QNFs would depend only on the parameters that characterize the black hole: its mass, charge and the angular momentum. This is reminiscent of an ordinary oscillator, whose frequency of oscillations would reveal important data regarding the force constant of the system, the coefficient of viscosity of the system (in the case of damped oscillations),etc. QNMs are significant astronomically as well, since they are expected to be detectable in various gravitational wave detectors being set up in different regions of the world. The recent observation of a transient gravitational wave signal by the LIGO group [132] is worth special mention here. The observed wave form reportedly matched extremely well with the predictions of GTR, but detectors to be set up in the future, having better accuracy, may reveal the presence of some discrepancy between GTR and observation, which can be resolved by more general modes of gravity.

In astronomy as well as astrophysics, the most important spacetimes are the asymptotically flat ones, the metrics describing which reduce to the Minkowski form in regions of spacetime free of the energy - momentum tensor. This is because we assume the large - scale structure of the spacetime of the universe to be largely flat, owing to the vast emptiness of the space between clumps of matter in the

observable universe. If the universe is indeed flat, then the QNMs of perturbations in asymptotically flat spacetimes could provide useful data regarding the structure of the spacetime.

In the case of asymptotically flat spacetimes themselves, the QNMs having very large imaginary parts (the highly damped ones) enjoy a special status, and are called asymptotic QNMs. They correspond to very large values of the mode number n and, in the case of four dimensional, asymptotically flat space times, take a form in which the real part of the QNF approaches a constant (equal to 0.0437123) and the imaginary part increases linearly with the mode number. These modes are important because of a possible connection between their constant real part and the quantized area of black hole event horizons.

According to Bekenstein [38], one of the pioneers of the field of black hole thermodynamics, the black hole horizon area A_n takes the form $A_n = n\gamma\ell_P^2$, ℓ_P being the Planck length, n is a natural number and the constant γ determines the size of the area quantum. In literature related to Loop Quantum Gravity, γ is called the Barbero - Immirzi parameter [134]. The value of γ is an important parameter that fixes the form of such theories and could provide crucial insight regarding quantized gravity. Using statistical arguments, the value of γ can be shown to take the form $\gamma = 4 \ln k$, where k is an undetermined integer. The connection between the horizon area and asymptotic QNFs comes from the ad - hoc proposal of Hod [39] to map the above - mentioned number, namely 0.0437123, to $\ln 3$ and thereby fix the value of k to 3. Hod's proposal is based on an appeal to a version of Bohr's correspondence principle, in which one argues that corresponding to a fundamental frequency in a classical system,

there exists an adiabatic invariant in the quantum mechanical system, having a quantized spectrum. In the case of black holes, the adiabatic invariant is usually taken to be the horizon area. Although such a connection between a numerically observed general form of asymptotic QNFs and a fundamental black hole parameter such as its area quantum may sound far - fetched, it has certainly attracted a lot of curiosity in the community and numerous works have been carried out, both to verify the original results of Hod and to extend the results to other dimensions as well [62].

It would certainly be interesting to see whether such a connection also exists in the case of generalized theories of gravity such as the Lovelock theory, and to see what form the expression for the quantized area spectrum would take in such theories. One would like to know how the area quantum depends on parameters like the dimension of the spacetime, the order of the theory, etc.

The above - mentioned facts signify the importance of QNMs in asymptotically flat black hole spacetimes. At the same time, there exists ample motivation for studying the QNMs of perturbations in other spacetimes as well. The other two types of solutions - the asymptotically de - Sitter (dS) and anti de - Sitter (AdS) - have also been studied extensively in recent times. dS and AdS spacetimes are solutions of Einstein's field equations that contain a non - zero cosmological constant Λ . Positive values of Λ correspond to dS and negative values to AdS spacetimes. As per some models such as the Λ CDM model, a non-zero Λ could prove useful in explaining the expanding Universe and hence could be relevant while discussing the long-term fate of the universe. If the matter density of the universe

is sufficiently large, then the universe will eventually collapse in on itself, and on the other hand, if the matter density is low, then there will be nothing to prevent an indefinite expansion of the universe.

1.4 AdS - CFT Correspondence and QNMs

The motivation for studying the QNMs in the asymptotically AdS case mainly stems from the gauge - gravity conjecture proposed by Maldacena [3] and Witten [89]. According to this conjecture, theories of gravity defined in an asymptotically AdS black hole spacetime of dimension n is dual to a strongly coupled field theory at finite temperature, defined in an $(n - 1)$ dimensional subspace; whereas pure AdS spacetime in n dimensions is dual to the field theory at absolute zero. What this means, roughly, is that there exists a one - to - one correspondence between parameters related to the black hole spacetime and parameters related to the field theory. Considering the $(n - 1)$ dimensional subspace as a “boundary” of the n dimensional “bulk” spacetime, we can observe that the dual relation between gravitation and CFT is very much similar to the way in which an interference pattern stored on the surface of a hologram stores information regarding the three dimensional structure of an object. For this reason, the gauge - gravity duality is also called “holographic correspondence”. It is also called the AdS - CFT correspondence, CFT standing for “Conformal Field Theory”.

According to the AdS - CFT correspondence, as mentioned above, a strongly coupled CFT at absolute zero is dual to a theory of grav-

itation defined in pure AdS spacetime of the next higher dimension, whereas a strongly coupled CFT at a finite temperature is dual to a theory of gravitation defined in an AdS spacetime containing a black hole. As mentioned before, such a duality means a one - to - one mapping between quantities related to the CFT and those related to gravitation. This enables us to calculate parameters related to the strongly coupled CFT by computing the corresponding parameter in the theory of gravitation. Because of the strong coupling, perturbative approaches fail in the case of the CFT, so that it is difficult to perform the computation of such parameters. On the other hand gravity is much weaker in comparison and the computation of the dual parameters is often a much simpler task.

One of such dualities between gauge theories and gravity is between a perturbation to an asymptotically AdS black hole spacetime and perturbations to a thermal state in the dual gauge theory. As an example of such a strongly coupled system, we can consider a quark - gluon plasma. According to the duality, such a system of quarks and gluons is dual to a black hole spacetime in the next higher dimension. Disturbing the black hole spacetime would then be dual to disturbing the plasma state. All such disturbances result in an oscillatory response, both in the case of the CFT and in the case of the black hole spacetime. In real - world situations, both of these oscillations are damped, characterized by complex frequencies of oscillations. In the case of a quark - gluon plasma system, the damped nature of the oscillations would be characterized by what is called a relaxation time, in which the oscillations would almost settle down to equilibrium. Such relaxation times are known to be related to the coefficient of damping, such as viscosity of the plasma. Viscosity is

an example of what are known as transport coefficients. Calculation of such transport coefficients, a difficult task to accomplish directly using QCD (which is the actual theory describing such plasma states) can be replaced by the much simpler task of finding the QNFs of the corresponding black hole perturbations, according to the AdS - CFT correspondence. The above - mentioned relaxation times are dual to the low - order QNFs. Such convenience has resulted in a lot of recent research activity on the behavior of physical fields in asymptotically AdS black hole spacetimes. It would be certainly of interest to know more about how the order of the gravitational theory affects the QNMs and thereby the relaxation times in the corresponding CFTs.

The horizon area spectrum of asymptotically AdS solutions also derive their physical significance from the gauge - gravity duality. Recent studies ([44–48] and references therein) suggest that the gravitational dual of the holographic entanglement entropy in quantum field theories is the area of minimal - area surfaces in AdS spaces. The entropy can be used to study phase transitions between various states of the field. An area - entanglement entropy relation of the form $S_A = \frac{Area(\gamma_A)}{4G_N^{(d-2)}}$ has been proposed [44, 49] which is very similar to the familiar area - entropy relation in the General Theory of Relativity. Here, γ_A is the d - dimensional minimal area surface in AdS_{d+2} and $G_N^{(d-2)}$ is the $(d + 2)$ - dimensional gravitational constant of the AdS gravity. Although the above relation was originally proposed for AdS spaces, it is equally applicable to any asymptotically AdS space, including one containing a black hole. In that case, the minimal surface tends to wrap the horizon and thus we can use the area of the event horizon in order to compute the entanglement entropy in the conformal field theory.

1.5 QNMs, Asymptotic QNMs and Gravitational Radiation in Higher Dimensions

An exhaustive survey of the vast literature on the evolution of various types of perturbations in different kinds of spacetimes would be too cumbersome to be carried out here, but the works mentioned in the following paragraphs provide a bird's - eye - view on the subject, in addition to providing an invaluable list of review materials on the same.

A detailed study on the asymptotic QNMs of Schwarzschild black holes in four and higher dimensions for gravitational, scalar and electromagnetic perturbations was carried out by Cardoso et al. [84]. The authors attempt to generalize the form of the asymptotic QNMs obtained earlier in the literature using numerical methods and to generalize the asymptotic form in the case of higher dimensions as well. The numerical results obtained by the authors for the case of electromagnetic perturbations are the first ones to be reported. The asymptotic limit of scalar and gravitational perturbations in five dimensions is seen to be of the form $\frac{\omega}{T_h} = \ln 3 + i(2n + 1)\pi$, ω and T_h being the QNF and the horizon temperature respectively and n is the mode number. It is also found that the corrections to the QNMs in the first order vary as $\frac{1}{n^{(d-3)/(d-2)}}$, d being the dimension of the spacetime.

Gravitational QNMs of higher dimensional Schwarzschild, Reissner - Nordstrom (RN), SdS and SAdS black holes in higher dimensional spacetimes were calculated by Konoplya [85] using the sixth order WKB method and the Horowitz - Hubeny method [37]. In the case

of asymptotically flat spacetimes, the QNMs were found to be inversely related to the horizon radius. For SdS black holes, the real and imaginary parts of the QNMs decrease with increasing values of the cosmological constant Λ , indicating a decreasing oscillational frequency and an increasing damping time. For SAdS black holes, however, a different sort of behavior is observed - the QNFs for SAdS black holes depend on the size of the black hole, being proportional to it in the case of large and intermediate - sized black holes. For very small black holes, it is found that the values of the QNFs reduce to those in pure AdS spacetimes. The behavior of these perturbations in higher dimensions was found to mimic that in the four dimensional case. Another notable feature observed this study is that the three kinds of perturbations - scalar, electromagnetic and gravitational - are not isospectral in higher dimensions, unlike the case in four dimensions. It would be interesting to investigate these behaviors in the case of higher dimensional, higher order theories such as the Lovelock model.

Zhang [87] has attempted to fix the Barbero - Immirzi parameter from the asymptotic form of QNFs for higher dimensional Schwarzschild - type black holes. The value of γ in the case of four dimensional Schwarzschild black holes was found to be $\gamma = \frac{\ln 3}{2\pi\sqrt{3}}$. In the case of higher dimensions, it was found that the parameter varies with the dimension d of the spacetime as $\gamma \propto \frac{1}{\sqrt{d}}$. Whether the value of γ in higher order theories would depend on the order of the theory would be worthwhile investigating.

The decay of charged scalar fields in RN and RN - AdS spacetimes was analyzed by Konoplya [86]. It was found that the real and imag-

inary parts of the QNFs increase with increase in the value of the charge of the field. Another interesting feature of the QNFs of these black holes is that, in the case of extremal and nearly extremal black holes, the values of the QNFs for neutral and charged scalar fields coincide.

1.6 Black Hole Thermodynamics and Black Hole Geometrothermodynamics

Black holes and thermodynamic systems behave similarly in many respects. To note just one example, we note that black holes in four dimensional spacetimes obey what is known as the Birkhoff's theorem, which roughly states that any black hole that is initially different from a spherically symmetric one will eventually settle down to a spherically symmetric configuration, characterized by just a handful of parameters. We can immediately see a similarity between this and the behavior of thermodynamic systems consisting of a large number of atoms. One does not need to specify the values of the position and momentum of each atom to know the thermodynamic states - the thermodynamic equilibrium states are characterized by just a few variables - temperature, pressure, etc.

Further justification for considering black hole spacetimes as thermodynamic systems is a similarity between the equations of gravity in black hole spacetimes and those of thermodynamics. This association between the two theories began with Bekenstein [38] who was the first one to observe that the area of the black hole horizon is a quantity that always increases for every kind of physical process that takes place in the vicinity of the black hole. This observation consti-

tutes one of the “laws of black hole thermodynamics”, which are four in number. These are summarized below:

1. Zeroth Law: Surface gravity of a stationary black hole is a constant. This is analogous to the Zeroth Law of thermodynamics, which states that the temperature is constant for system in equilibrium with the surroundings.
2. First Law: $dM = \frac{\kappa}{8\pi G}d\mathcal{A}$, M being the black hole mass, κ the surface gravity, G the Newton’s gravitational constant. This is analogous to the first law of thermodynamics, namely $dE = TdS$, E , T and S being the energy of the system, its temperature and the entropy, respectively. In the case of a charged, rotating black hole, the corresponding expression becomes: $dE = TdS + \Phi dQ + \Omega dJ$, Q , J , Φ and Ω being the charge of the black hole, the horizon angular momentum, horizon electrostatic potential and the horizon angular velocity, respectively.
3. Second Law: $d\mathcal{A} \geq 0$, which is analogous to $dS \geq 0$ in ordinary thermodynamics.
4. Third Law: The Third Law of Thermodynamics states that it is impossible by any process, no matter how idealized, to reduce the entropy of a system to its absolute-zero value in a finite number of operations. In the context of black hole systems, this would mean that the surface gravity of a black hole can never attain zero value through any physical process involving the horizon.

The laws stated above contain the most important associations between thermodynamic variables and black hole parameters.

A closer inspection of the laws, however, reveal some pitfalls that one may encounter by taking these laws and the associated links between thermodynamic and black hole parameters too literally without taking into account the coordinate - frame - dependent - nature of many black hole parameters. One such point that warrants caution is the zeroth law itself, which links the dynamic variable called specific gravity of the black hole surface (called surface gravity) and the thermodynamic variable called temperature. The problem arises from the fact that the surface gravity, which is the force (per unit mass), as measured by an asymptotic observer, necessary to hold a particle at the horizon, is frame - dependent. This is in the sense that, while the surface gravity may be finite as per the asymptotic observer, an infalling, accelerating observer can not escape from the horizon. Therefore, as per his/her measurement, the necessary force will appear to diverge, along with the temperature.

Along with this discrepancy is the fact that the traditional picture of a black hole as a body from the gravitational influence of which nothing can escape is directly at odds with the zeroth law, which associates a temperature with it, making it “the ideal black body at a finite temperature”, and requiring it to possess a thermal radiation, which is nowadays called Hawking radiation [74]. Yet another point of potential conflict between the ordinary and black hole laws of thermodynamics, that tell us that they indeed describe different types of physical systems, comes from inspecting the second law. Although positively correlated as per the second law, the horizon area and the entropy vary dimensionally, unless modified with suitable prefactors as per the first law. The thermodynamic entropy is dimensionless by definition, while the area is not. The presently accepted, dimension-

less form of the area law in 4D spacetime is given by,

$$S = \frac{k_B c^3}{4G\hbar} \mathcal{A} = \frac{k_B}{4} \frac{\mathcal{A}}{\ell_P^2},$$

ℓ_P representing the Planck length, a length constructed out of G , \hbar and c , the assumed scale of length at which the effects of quantum gravity become apparent. As noted earlier, it is interesting to note that the dimensionless entropy is proportional to the area of the black hole, rather than its volume, like in ordinary statistical mechanics. In fact, it may have been one of the early indications of the duality between lower dimensional field theories and higher dimensional gravity.

In addition to the study of such analogies is another important question - that of the thermodynamic stability of a black hole. The thermodynamic stability of a black hole is a concept that is similar to that of some phase of matter - as long as the phase does not change with change in some thermodynamic parameter like the temperature of the system, the phase is said to be thermodynamically stable. Mathematically, such stable phases are associated with a positive value of the specific heat (at constant pressure) C_p . When, however, the value of C_p is negative, it signals an unstable phase. Thermodynamic transitions between macroscopically distinguishable stable phases are accompanied by discontinuities in C_p when expressed as functions of the temperature T of the system. During a phase transition, some thermodynamic potential function such as the free energy F of the system becomes non - analytic. In general, during what is known as an n^{th} order phase transition, the n^{th} derivative of the thermodynamic potential will be non analytic. Thus, for a first order phase transition, the free energy itself may remain analytic with the

first derivative being non analytic at the critical value of the control parameter such as T ; for a second order phase transition, F and its first derivative may remain analytic with non - analyticity in the second derivatives, etc.

When one deals with black hole thermodynamics, the usual recipe for assessing the thermodynamic stability is as follows: one starts with a static, spherically symmetric black hole spacetime whose metric takes a form similar to $ds^2 = -f(r)dt^2 + \frac{1}{f(r)}dr^2 + \dots$ in which the lapse function $f(r)$ may depend on the black hole parameters such as the mass M , charge Q and the angular momentum J . Next, M , Q , J and thermodynamic parameters such as T are expressed in terms of the black hole event horizon r_h using the identity

$$T(r_+) = \frac{1}{4\pi\kappa_B} \left. \frac{df}{dr} \right|_{r=r_+}$$

In order to assess the thermodynamic stability, we have to compute the specific heat C_p for the spacetime.

The specific heat C_p of the black hole may be calculated by using the relation

$$C_p(T) = \frac{\partial M}{\partial T}$$

In many spacetimes that are usually encountered, the temperature, entropy, etc. are found to be monotonic functions of the horizon radius r_h . In such cases, it may be more convenient to find C_p as a function of r_h directly instead of T . If that is the case, one can make use of the relation $C_p(r_h) = \frac{\partial M}{\partial T} = \frac{\partial_{r_h} M}{\partial_{r_h} T}$. One can then test for non - analytic behavior of C_p either analytically or using graphical methods. The graphical methods come especially handy in situations where the actual expression for C_p in terms of T or r_h turns out to

be too complicated to handle manually. Whatever the method, the presence of such non analytic points in the domain of C_p will signal the presence of second order phase transitions in the corresponding black hole spacetime. The question as to what exactly undergoes the transition, however, will only be clear once complete quantization of gravity becomes a reality.

While discussing the similarity between black holes and thermodynamic systems, it is worthwhile to note that the analogy also hints at a connection between gauge theories and gravity, explained in the previous sections under AdS - CFT correspondence. We know that the entropy of the event horizon, at least in four dimensions, is proportional to its area. For a thermodynamic system, however, the statistical entropy is proportional to the volume of the system instead of the area. Thus, a four dimensional black hole can not correspond to a four dimensional thermodynamic system. However, we also note that “area” in a five dimensional spacetime is equivalent to “volume” in a four dimensional spacetime. Thus, if a four dimensional thermodynamic system has any correspondence with a gravitational system at all, then the gravitational system must exist in a spacetime of five dimensions - the same deduction as that obtained from the AdS - CFT correspondence.

1.7 Black Hole Thermodynamic Geometry

Thermodynamic geometry is essentially the utilization of the methods of differential geometry in order to study the thermodynamic behavior of systems. The core concept behind thermodynamic geometry is identifying the thermodynamic phase space of a system with a Riemannian manifold. An equilibrium state of such a thermodynamic

system would be characterized by a state equation, which would then define a surface in the manifold. The critical points corresponding to phase transitions are identified with extremal points on the surface. Since different points on the surface represent different states at which the system can be in equilibrium, curves on the surface would naturally represent transitions between states. The methods of analytical and differential geometry could then be employed in order to analyze such transitions.

In thermodynamic geometry, such a Riemannian manifold is endowed with a metric called the thermodynamic metric. The components of the metric tensor are given by the partial derivatives of some thermodynamic potential Φ such as the free energy F of the black hole system with respect to some control parameter, such as the horizon temperature T , the horizon radius r_h , etc. (A thermodynamic potential is a function obtained by Legendre transformation of the fundamental relation of the thermodynamic system. For example, $F = E - TS$, where E , T and S are the energy of the system, the temperature and the entropy, respectively.) Different choices of the thermodynamic potential are known as different representations in the vocabulary of thermodynamic geometry. For example, the choice of E gives the energy representation, the choice of S is called entropy representation, etc. We can obtain a thermodynamic curvature that is independent of the choice of the potential by defining what is known as a Legendre invariant thermodynamic metric and using it to calculate the curvature. In general, such an invariant metric g defined in terms of a thermodynamic potential Φ with a set of control parameters E^c has components of the form

$$g_{ad} = \left(E^c \frac{\partial \Phi}{\partial E^c} \right) \left(\eta_{ab} \delta^{bc} \frac{\partial^2 \Phi}{\partial E^c \partial E^d} \right) \quad (1.12)$$

,

where η and δ represent the Minkowski metric and the Kronecker delta respectively. In the case of black hole spacetimes, the black hole mass M plays the role of the energy of the system. Also, the horizon radius r_h is also taken as the control parameter and all other quantities such as Φ are expressed in terms of r_h .

The use of Riemannian geometry in the study of statistical mechanics and thermodynamics, in terms of a metric in local coordinates, assigned to the manifold, date back to Rao[111]. The metric would allow us to compute the curvature scalar for the manifold, which would then be identified with thermodynamic interaction between states. What this means is that zero curvature of the manifold would represent a system at equilibrium, having absolutely zero interaction with the surroundings. On the other hand, parts of the manifold with non zero curvature would represent states that would essentially be thermodynamically unstable, representing potential interactions including phase transitions. In particular, second order phase transitions would be signaled by divergences in the curvature.

Although the essential idea behind the methods of thermodynamic geometry has not undergone considerable change since its inception, so can not be said about that actual metric that is to be associated with the phase space. The components of the metric are usually defined as partial derivatives of thermodynamic potential functions

with respect to control parameters such as the temperature, horizon radius, etc. The control parameters are collectively represented as N_a . Usual choices for the thermodynamic potentials are the mass M , internal energy U , entropy S , etc. of the black hole spacetime. Depending on the choice of the metric, different versions of the geometric approach exist. The use of thermodynamic geometry in the space of equilibrium states was first performed by Weinhold[117] and Ruppeiner [118]. Weinhold proposed a metric structure in the energy representation as $g_{ij}^W = \partial_i \partial_j M(U, N^a)$, while Ruppeiner defined the metric structure as $g_{ij}^R = -\partial_i \partial_j S(U, N^a)$. Components of these metrics are those of the Hessian matrix of the internal energy M and the entropy S respectively, with respect to the extensive thermodynamic variables N^a . Weinhold's metric was found to be conformally connected to Ruppeiner's through the relation $ds_R^2 = \frac{ds_W^2}{T}$ [123], T being the horizon temperature. Ruppeiner's metric has extensively been used in the geometric analysis of various black hole spacetimes[124]. Recently, Quevedo et al.[120] presented a new formalism called geometrothermodynamics, which allows us to derive Legendre invariant metrics for the phase space. Geometrothermodynamics presents a unified geometry where the metric structure describes various types of black hole thermodynamics [119–122, 125–130].

1.8 Structure of the Thesis

Motivated by the arguments put forward in the preceding paragraphs, this thesis summarizes some basic theoretical investigations into the dynamics of fields in, and thermodynamic behavior of, black hole spacetimes in the Lanczos - Lovelock model of gravity. The dynamics of fields is studied by analyzing their quasinormal frequencies.

We find out how the quasinormal frequencies change when we treat the dimension d and order k as variable parameters. The thermodynamics is studied by calculating the specific heat of the spacetime and looking for divergences in order to find out potential transition points. A calculation of the thermodynamic curvature also corroborates the occurrence of such phase transitions. The thesis is organized into five chapters:

Chapter 1: In this chapter, we emphasize the importance of studying black hole physics in higher dimensions. We briefly discuss the peculiarities of black holes existing in higher dimensional spacetimes, and the effects of higher dimensions on the horizon structure, stability and dynamics of black holes, etc. We also go through higher order models of gravity, along with existing ideas about their advantages and disadvantages. We finally come to a discussion of the Lanczos - Lovelock (LL) model of gravity, explaining the structure of the LL Lagrangian, the form of the field equation and the form of the static, spherically symmetric solutions of the theory. We also briefly discuss fundamental ideas of black hole thermodynamics and thermodynamic geometry.

Chapter 2 : Chapter 2 deals with the modes of evolution of massless scalar fields in the asymptotically AdS spacetime surrounding maximally symmetric black holes of large and intermediate size in the Lovelock model. The QNMs are calculated using the Horowitz - Hubeny numerical method. It is observed that the modes are purely damped at higher orders. Also, the rate of damping is seen to be independent of order at higher dimensions. The asymptotic form of these frequencies for the case of large black holes is found analytically. Finally, the area spectrum

for such black holes is deduced from these asymptotic modes, invoking the Ehrenfest Principle for the black hole spacetime.

Chapter 3 : Chapter 3 is devoted to the computation of the quasinormal modes of metric perturbations in asymptotically flat black hole spacetimes in the Lovelock model for different spacetime dimensions and higher orders of curvature. It is analytically established that in the asymptotic limit $l \rightarrow \infty$, the imaginary parts of the quasi normal frequencies become constant for tensor, scalar as well as vector perturbations. Numerical calculation using the WKB method shows that this indeed is the case. Also, the real and imaginary parts of the quasinormal modes are seen to increase as the order of the theory k increases. The real part of the modes decreases as the spacetime dimension d increases, indicating the presence of lower frequency modes in higher dimensions. Also, it is seen that the modes are roughly isospectral at very high values of the spacetime dimension d .

Chapter 4 : In Chapter 4, we investigate the thermodynamic behavior of maximally symmetric charged, asymptotically AdS black hole solutions of Lovelock gravity. We explore the thermodynamic stability of such solutions by the ordinary method of calculating the specific heat of the black holes and investigating its divergences which signal second order phase transitions between black hole states. We then utilize the methods of thermodynamic geometry of black hole spacetimes in order to explain the origin of these points of divergence. We calculate the curvature scalar corresponding to a Legendre - invariant thermodynamic metric of these spacetimes and find that the divergences in the black hole specific heat correspond to sin-

gularities in the thermodynamic phase space. We also calculate the area spectrum for large black holes in the model by applying the Bohr - Sommerfeld quantization to the adiabatic invariant calculated for the spacetime.

Chapter 5 : Chapter 5 includes the summary of the findings from the studies that this thesis is a record of.

2

Scalar Field Evolution and Area Spectrum for Lovelock-AdS Black Holes

2.1 Introduction

Gauge-gravity dualities like the AdS/CFT correspondence [3] make it possible to study the properties of conformal fields in a particular dimension d by studying the evolution of fields in a black hole spacetime that is asymptotically AdS in $(d + 1)$ dimensions and this has led to considerable interest in the study of asymptotically AdS black hole spacetimes. The main difficulty in studying field evolution in such spacetimes is that the stability of the spacetime against perturbations is not always guaranteed, unlike in the case of asymptotically flat spacetimes in first order theories in four dimensions. The instability of linear perturbations in higher-order and higher dimensional theories has already been investigated [22, 28, 29]. The instability also extends to the thermodynamics of the black hole when we consider AdS spacetimes, with the well-known Hawking-Page phase transitions [30] signaling a transition between the black hole spacetime and thermal AdS spacetime. Recent studies [10, 13, 19] on the Lovelock model have confirmed the existence of dynamic instability against metric perturbations in asymptotically flat black hole space-

times. Dynamic instability means that the solutions to the equation for the metric perturbation become unstable outside the event horizon for large values of their eigenvalue. This instability exists for all types of metric perturbations-tensor, vector and scalar. These instabilities occur when the mass of the black hole falls below a lower critical bound that depends on the coupling constants, the dimension of the spacetime and the order of the theory [19].

Quasi normal modes are damped oscillations (having complex frequencies), known to dominate the intermediate stage of the evolution of small perturbations of a black hole spacetime and have been studied extensively. Detailed reviews and methods of calculation of quasi normal modes are found in numerous papers that include [31–36]. Quasi normal modes are known to depend only on the parameters of the black hole, such as mass, charge and angular momentum, and be completely independent of the type of the agent that caused it. These modes are obtained as the solution of the respective field equation, when solved with respect to the metric that describes the particular black hole spacetime of interest. In the case of asymptotically flat spacetimes, the effective potential that is perceived by the field in the spacetime often resembles a finite potential barrier such that the potential vanishes at infinity. This leads to the possibility of obtaining solutions that are purely ingoing at the event horizon of the black hole and purely outgoing at infinity, both resembling plane waves when expressed in terms of a scaled co-ordinate called the tortoise co-ordinate. These modes may be observed in the future with the aid of gravitational detectors. In the case of asymptotically AdS spacetimes, however, the potential grows indefinitely at infinity. Therefore, one usually looks for solutions that vanish at infinity,

while the boundary conditions at the event horizon remain unchanged [37]. This is motivated by the case of pure AdS spacetime, where the potential effectively confines the field as if “in a box” and solutions exist only with a discrete spectrum of real frequencies. Even though black holes in asymptotically AdS spacetimes are not believed to exist in nature, interest in studying their quasi normal modes stems from the above-mentioned AdS/CFT correspondence [3]. According to the AdS/CFT correspondence, these perturbations correspond to perturbations of the thermal state of the strongly coupled conformal field at the boundary of the spacetime and the quasi normal modes correspond to the return to thermal equilibrium, so that the quasi normal frequencies give a measure of the time scale for the relaxation, which is difficult to compute directly. This provides the motivation to study the quasi normal modes of various fields in asymptotically AdS spacetimes. Earlier works on the quasi normal modes of Schwarzschild-AdS black holes [37] have proved that the modes scale with the temperature of the event horizon.

Complete quantization of gravity is one of the major goals of physics. Despite decades of research by physicists all over the world, it is yet to be achieved with complete success. One often takes clues from the classical theory of a system when attempting its quantization and gravity needs to be no different. Quantization of the black hole horizon area is expected to be a major feature of any successful quantum theory of gravity. The original “classical” theory of gravity, namely the General Theory of Relativity (GTR) does provide us with the tools necessary to estimate the value of the area quantum. It is known from field theory that the presence of a periodicity in the classical theory of a system points to the existence of

an adiabatic invariant with a discrete spectrum in the corresponding quantum theory. Interestingly, it has been observed in GTR that the numerical value of these frequencies, in the limit of “large” frequencies, follow a distinct pattern, with the real part approaching a fixed value. These are termed asymptotic frequencies. Suggestions have been made that the fixed value of the real part can be viewed as a physically relevant periodicity in the (classical) black hole system which would then lead to the existence of certain adiabatic invariant quantity, which in turn would possess equally spaced spectrum according to Bohr-Sommerfeld quantization. Once we read it together with Bekenstein’s original proposal [38] that the black hole entropy is an adiabatic invariant with a discrete, equally spaced spectrum, we come to the conclusion that the entropy spectrum (and, by extension, the area spectrum) can be deduced from the asymptotic value of the quasi normal frequencies. The connection between the fixed asymptotic frequencies and the quantized area spectrum was made by Hod [39]. Dreyer [42] recovered Hod’s result in the Loop Quantum Gravity. A new interpretation for the quasi normal modes $\omega = \omega_R + i\omega_I$ of perturbed black holes as equivalent to that of a collection of damped harmonic oscillators with real frequency $\omega_0 = \sqrt{\omega_R^2 + \omega_I^2}$ was introduced by Maggiore [43] and used in conjunction with Hod’s method in order to compute the area spectrum of Schwarzschild black holes.

As with the case of quasi normal modes, it is the AdS/CFT correspondence that provides the motivation for studying the area spectrum of black holes in asymptotically AdS spacetimes. Recent studies ([44–48] and references therein) suggest that the gravitational dual of the holographic entanglement entropy in quantum field theories is the area of minimal-area surfaces in AdS spaces. The entropy can be

used to study phase transitions between various states of the field. An area-entanglement entropy relation of the form $S_A = \frac{Area(\gamma_A)}{4G_N^{(d-2)}}$ has been proposed [44, 49] which is very similar to the familiar area-entropy relation in General Theory of Relativity. Here, γ_A is the d -dimensional minimal area surface in AdS_{d+2} and $G_N^{(d-2)}$ is the $(d+2)$ -dimensional gravitational constant of the AdS gravity. Although the above relation was originally proposed for AdS spaces, it is equally applicable to any asymptotically AdS space, including one containing a black hole. In that case, the minimal surface tends to wrap the horizon and thus we can use the area of the event horizon in order to compute the entanglement entropy in the conformal field theory.

In this chapter, we numerically compute the quasi normal frequencies for massless scalar field perturbations in asymptotically AdS, spherically symmetric spacetimes in Lovelock model using the metric derived in [50]. We analytically find out the asymptotic form of the frequencies following [51] and use it to deduce the area spectrum of large black holes in the model. A brief outline of the chapter is as follows: in Sect. 2.2, we explain the maximally symmetric Lovelock model and the resulting metric for the spacetime as given in [50]. Details of the Horowitz-Hubeny numerical method of computing the quasi normal frequencies in AdS black hole spacetimes to the case of massless scalar fields in the vicinity of such a black hole in the Lovelock-AdS model are also given in the same section. The results of the numerical procedure are presented and analyzed in Sect. 2.3. In Sect. 2.4, we analytically determine the asymptotic quasi normal frequencies of the field for the case of large black holes following [51]. The results of that analysis are used in order to find the area spectrum of the black hole using the Kunstatter's method [52] in Sect.

2.4.1. The results are summarized in Sect. 3.4.

2.2 The Metric and the Numerical Computation of Quasinormal Frequencies

The Lovelock model [145] is considered to be the most natural generalization of GTR. The Lovelock Lagrangian is a polynomial which consists of dimensionally continued higher order curvature terms. The most striking property of this Lagrangian is that it yields field equations that are in second order in the metric although the Lagrangian itself may contain higher order terms. Also, the theory is known to give solutions that are free of ghosts. The maximum order of terms in the action, k , is fixed by the number of dimensions of the space-time d in Lovelock model according to the relation $k = \lfloor \frac{d-1}{2} \rfloor$ where $\lfloor x \rfloor$ denotes the integer part of x . The action I_G is written as,

$$I_G = \kappa \int \sum_{p=0}^k \alpha_p L^{(p)}, \quad (2.1)$$

where α_p are arbitrary (positive) coupling constants, and $L^{(p)}$, given by

$$L^{(p)} = \epsilon_{a_1 \dots a_d} R^{a_1 a_2} \dots R^{a_{2p-1} a_{2p}} e^{a_{2p+1}} \dots e^{a_d}, \quad (2.2)$$

is the p^{th} order dimensionally continued term in the Lagrangian, R^{ab} represents the Riemann curvature and e^a represents the vielbein. $\epsilon_{a_1 \dots a_d}$ is the Levi-Civita symbol in d dimensions. κ is a parameter related to the k^{th} gravitational constant G_k by the expression $\kappa = \frac{1}{2(d-2)! \Omega_{d-2} G_k}$, Ω_{d-2} being the volume of the $(d-2)$ dimensional spherically symmetric tangent space with unit curvature.

The difficulty with the Lagrangian given above, with arbitrary values for α_p , is that it becomes very difficult (if not impossible) to study the evolution of fields, since it is not at all clear whether the operator representing the evolution is Hermitian or not. As mentioned in the previous section, this problem, for the case of metric perturbations, has been analyzed in [19]. Although a general instability depending on the black hole mass has been established in that work, the numerical value for the critical mass has not been calculated. Also, it is very difficult to predict whether the presence of a cosmological constant raises or lowers the critical mass, as long as we consider a model with arbitrary α_p . Moreover, for the same case, the existence of negative energy solutions with horizons and positive energy solutions with naked singularities for (2.1) has been pointed out earlier [53, 54]. These difficulties bring out the necessity of selecting suitable values for the coupling coefficients in order to have models that support maximally symmetric solutions and external perturbations. Maximally symmetric solutions to Lovelock model have long been known [50], which are derived by requiring that the theories must possess a unique cosmological constant (and consequently a unique AdS radius R) for all orders. The resulting set of coupling constants are seen to be labeled by the order k and the gravitational constant G_k . The metric describing the spherically symmetric black hole spacetime is derived from the action given in (2.1) with the choice

$$\alpha_p = \begin{cases} \frac{R^{2(p-k)}}{(d-2p)} \binom{k}{p} & , p \leq k \\ 0 & , p > k \end{cases} \quad (2.3)$$

where $1 \leq k \leq \lfloor \frac{d-1}{2} \rfloor$. The resulting field equations are of the form

$$\epsilon_{ba_1 \dots a_{d-1}} \bar{R}^{a_1 a_2} \dots \bar{R}^{a_{2k-1} a_{2k}} e^{a_{2k+1}} \dots e^{a_{d-1}} = 0 \quad (2.4)$$

$$\epsilon_{aba_3 \dots a_d} \bar{R}^{a_3 a_4} \dots \bar{R}^{a_{2k-1} a_{2k}} T^{a_{2k+1}} e^{a_{2k+2}} \dots e^{a_{d-1}} = 0 \quad (2.5)$$

Here, $\bar{R}^{ab} := R^{ab} + \frac{1}{R^2} e^a e^b$. Such theories are labeled by k and have two fundamental constants, κ and R , related to the gravitational constant G_k and the cosmological constant Λ respectively through the relations

$$\kappa = \frac{1}{2(d-2)! \Omega_{d-2} G_k}, \quad (2.6)$$

$$\Lambda = -\frac{(d-1)(d-2)}{2R^2}, \quad (2.7)$$

Ω_{d-2} being the volume of the $(d-2)$ dimensional spherically symmetric tangent space. The static and spherically symmetric solutions to (2.4), written in Schwarzschild-like coordinates, take the form

$$ds^2 = -f(r)dt^2 + \frac{dr^2}{f(r)} + r^2 d\Omega_{d-2}^2, \quad (2.8)$$

where $f(r)$ is given by

$$f(r) = 1 + \frac{r^2}{R^2} - \sigma \left(\frac{C_1}{r^{d-2k-1}} \right)^{1/k}. \quad (2.9)$$

We take $\sigma = 1$. The integration constant C_1 is written as

$$C_1 = 2G_k(M + C_0), \quad (2.10)$$

where M stands for the mass of the black hole. The constant C_0 is chosen so that the horizon shrinks to a point for $M \rightarrow 0$, as

$$C_0 = \frac{1}{2G_k} \delta_{d-2k,1}. \quad (2.11)$$

It is interesting that the exponent of $(\frac{1}{r})$ in (4.2) is proportional to $(d - 2k - 1)$. Since $k = [\frac{d-1}{2}]$, $(d - 2k - 1) = 0$ in odd dimensions and $(d - 2k - 1) = 1$ in even dimensions. Thus the solution in even dimensions resemble the Schwarzschild-AdS solution. The $(d - 2k - 1) = 0$ cases correspond to Chern-Simmons theories which have a vacuum that is different from AdS [50]. Their quasi normal modes, mass and area spectra have already been computed [55]. What makes it interesting is the fact that recent studies [19] on the stability of metric perturbations in Lovelock model also point out that it is possible to predict the (in)stability of the perturbations only in even dimensions. The present work is limited to the cases where $d - 2k - 1 \neq 0$. Then we have $C_0 = 0$ and $C_1 = 2G_k M$. Consider the scalar field $\Phi(r, t, x_i)$ that obeys the Klein-Gordon equation given by

$$\frac{1}{\sqrt{g}} \partial_A \sqrt{g} g^{AB} \partial_B \Phi = 0, \quad (2.12)$$

x_i being the co-ordinates in the spherically symmetric tangent space and g_{AB} being components of the metric tensor. We impose the boundary conditions of ingoing plane wave solution at the event horizon and vanishing field at the boundary. The boundary condition at the horizon suggests the ansatz $\Phi = e^{-i\omega(t+r_*)}$ where r_* is the tortoise coordinate defined by

$$dr_* = \frac{dr}{f(r)}. \quad (2.13)$$

In the $(v = t + r_*, r)$ system, the metric reads

$$ds^2 = -f(r)dv^2 + 2dvdr + r^2 d\Omega_{d-2}^2, \quad (2.14)$$

and we take the ansatz

$$\Phi(v, r, x_i) = r^{\frac{2-d}{2}} \psi(r) Y(x_i) e^{-i\omega v}, \quad (2.15)$$

so that (2.12) becomes

$$f(r) \frac{d^2}{dr^2} \psi(r) + [f'(r) - 2i\omega] \frac{d}{dr} \psi(r) - V(r) \psi(r) = 0, \quad (2.16)$$

with the effective potential

$$V(r) = \frac{(d-2)(d-4)}{4r^2} f(r) + \frac{d-2}{2r} f'(r) + \frac{l(l+d-3)}{r^2}. \quad (2.17)$$

Here, l represents the eigenvalue of the operator on the LHS of (2.12) acting on the functions $Y(x_i)$ in the spherically symmetric tangent space. In order to numerically calculate the quasi normal frequencies for (2.16), we expand the field Φ as a power series about the horizon and impose the vanishing boundary condition at infinity. We change the variable from r to $x = \frac{1}{r}$ in order to map the range $r_+ < r < \infty$ to a finite range. In terms of x , (2.16) becomes

$$s(x) \frac{d^2}{dx^2} \psi(x) + \frac{t(x)}{x-x_+} \frac{d}{dx} \psi(x) + \frac{u(x)}{(x-x_+)^2} \psi(x) = 0, \quad (2.18)$$

where

$$\begin{aligned} s(x) &= -x^4 f(x), \quad t(x) = -x^4 f'(x) - 2x^3 f(x) - 2i\omega x^2, \\ u(x) &= (x-x_+) V(x), \end{aligned} \quad (2.19)$$

and

$$V(x) = \frac{(d-2)(d-4)x^2 f(x)}{4} - \frac{(d-2)x^3 f'(x)}{2} + l(l+d-3)x^2. \quad (2.20)$$

In the numerical procedure, we find out the coefficients of the expansion of the functions $s(x)$, $t(x)$ and $u(x)$ as power series in $(x - x_+)$ using a computer with s_i , t_i and u_i denoting the coefficient for the i^{th} term in the expansion of the respective functions. Then an expansion for $\psi(x)$ of the form

$$\psi(x) = \sum_{n=0}^{\infty} a_n (x - x_+)^n, \quad (2.21)$$

is substituted into (2.18) which yields

$$a_n = -\frac{1}{P_n} \sum_{k=0}^{n-1} [k(k-1)s_{n-k} + kt_{n-k} + u_{n-k}]a_k, \quad (2.22)$$

where

$$P_n = n(n-1)s_0 + nt_0. \quad (2.23)$$

We fix a_0 and numerically calculate the coefficients in (2.19) and (2.22) to different orders and compute the value of the field $\psi(x)$ as given in (2.21). ω will appear as a parameter in the expression for $\psi(x)$. Since we wish to impose the boundary condition of vanishing field at infinity, we solve the equation $\psi(0) = 0$ for ω . It is observed, by comparison with the values in [37], that the quasi normal frequencies are one of the solutions of the equation $\psi(0) = 0$, solved for ω , after ψ has been computed using (2.21) for some reasonably high value of n , which should be fixed by trial and error. We assume the same to be true in higher orders as well and look for the value of the quasi normal modes among the set of discrete values of ω that are obtained. For each value of ω obtained, we evaluate the absolute value of the LHS of (2.18) at a point close to the event horizon, since we have assumed plane wave solutions there. We choose that value of ω as the

quasi normal frequency for which the absolute value comes closest to zero (the assumption here is that (2.21) is satisfied exactly only for the quasi normal frequency, which we seek, and not by other roots of $\psi = 0$.) We increase the number of terms to which $\psi(x)$ and the coefficients are calculated until the required precision is attained.

2.3 Discussion on Results of the Numerical Calculation

We implement the procedure outlined above after fixing the value of the constants a_0 and R to 1. We investigate the quasi normal frequencies of large ($r_h \gg R$) and intermediate ($r_+ \sim R$) black holes and set $\omega = \omega_R - i\omega_I$ as done in [37] since we are interested in damped modes. As mentioned before, the analysis is limited to the cases where $d - 2k - 1 \neq 0$. The results for the lowest ($l = 0$) modes of the massless scalar field for first order theories have been summarized in TABLE 2.1. TABLE 2.2 contains the same for higher orders. Figures 2.1 to 2.6 show the results in detail. As evident from Figure 2.1 and Figure 2.2, both ω_R and ω_I show linear dependence on r_+ for the case of large black holes in first order theories. The linearity seems to be broken when we move to the intermediate-sized black holes, the results for which have been plotted in Figure 2.3 and Figure 2.4. Although the plots for intermediate-sized black holes look linear, the $\omega_R - r_+$ dependence for their case rather resembles an $(x, y = x + \frac{1}{x})$ relation. The temperature of the event horizon for the metric (4.1), given by

$$T = \frac{1}{4\pi\kappa_B k} \left((d-1) \frac{r_+}{R^2} + \frac{d-2k-1}{r_+} \right), \quad (2.24)$$

where κ_B denotes the Boltzmann's constant, also depends on r_+

Table 2.1: Variation of the frequency of the lowest ($l = 0$) massless ($m = 0$) mode for first order theories.

	$d = 4, k = 1$		$d = 5, k = 1$		$d = 6, k = 1$	
r_+	ω_R	ω_I	ω_R	ω_I	ω_R	ω_I
100	184.958	-266.392	311.785	-274.542	412.327	-272.185
50	92.496	-133.196	155.919	-137.268	206.194	-136.088
10	18.608	-26.642	31.351	-27.432	41.434	-27.187
5	9.471	-13.326	15.935	-13.683	21.146	-13.386
3	5.916	-8.001	9.921	-8.161	13.015	-8.044
2	4.235	-5.340	7.062	-5.376	9.164	-5.223

in the same manner. Since $(x, y = x + \frac{1}{x}) \sim x$ for large x , we conclude that both ω_R and ω_I scale with the temperature for large as well as intermediate-sized black holes for first order theories, in agreement with earlier works [37]. Another observation is that ω_I seems to be independent of dimension d in first order theories. When we consider higher order theories, the numerical results for which have been plotted in Figure 2.5 and Figure 2.6, we observe that all modes are purely damped ones. We have only plotted ω_I vs r_+ in the case of higher order theories for this reason. There, we observe that, both for large and intermediate-sized black holes, ω_I is independent of the order of the theory when the dimension d stays the same.

Table 2.2: Variation of the frequency of the lowest ($l = 0$) massless ($m = 0$) mode in higher orders.

	$d = 6, k = 2$		$d = 7, k = 2$		$d = 8, k = 2$		$d = 8, k = 3$	
r_+	ω_R	ω_I	ω_R	ω_I	ω_R	ω_I	ω_R	ω_I
100	0	-595.081	0	-1013.063	0	-1593.741	0	-1593.762
50	0	-357.045	0	-506.450	0	-796.796	0	-796.839
10	0	26.642	0	-101.185	0	-159.019	0	-159.205
5	0	-29.776	0	-50.523	0	-79.193	0	-79.467
3	0	-17.938	0	-30.354	0	-47.368	0	-47.623
2	0	-12.105	0	-20.475	0	-31.807	0	-31.831

2.4 Asymptotic Quasinormal Modes and Area Spectrum of Large Black Holes

We analytically find the asymptotic form of the quasi normal frequencies in the large black hole limit following the method of perturbative expansion of the wave equation in the dimensionless parameter ω/T_H that has earlier been employed in the case of d -dimensional SAdS black holes [51]. Here, T_H is the Hawking temperature of the horizon and ω is the frequency of the mode. We take the metric to be of the form given in (4.1). For large black holes, the metric gets approximated as,

$$ds^2 = \hat{f}(r)dt^2 + \frac{dr^2}{\hat{f}(r)} + r^2 ds^2(\mathbb{E}^{d-2}), \quad (2.25)$$

with

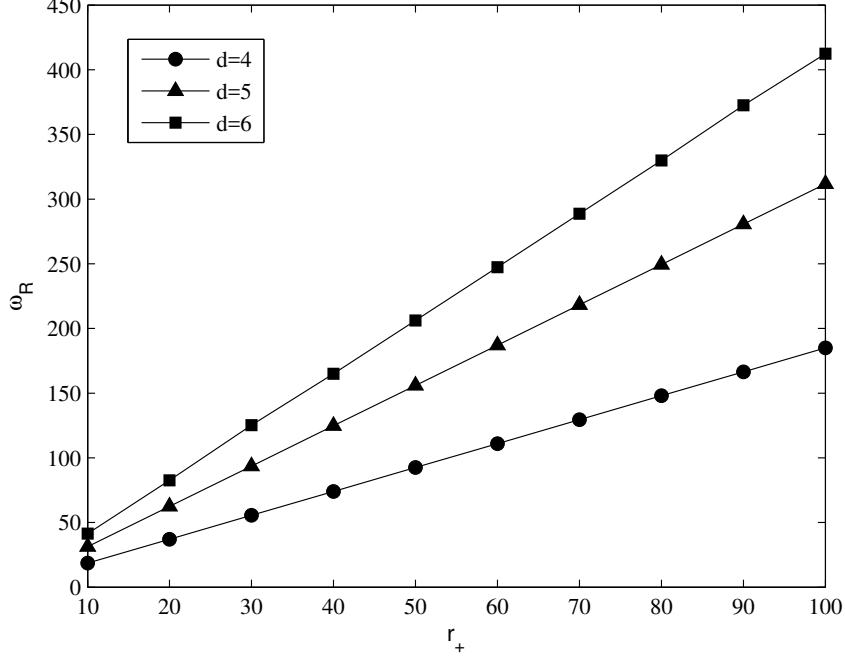


Figure 2.1: ω_R vs r_+ plot for large black holes in first order theories

$$\hat{f}(r) = \frac{r^2}{R^2} - \left(\frac{2G_k M}{r^{d-2k-1}} \right). \quad (2.26)$$

It is easily seen that the event horizon is given by

$$r_h = R \left[\frac{2G_k M}{R^{d-2k-1}} \right]^{\frac{1}{d-1}}. \quad (2.27)$$

In terms of the new metric (2.25), the Klein-Gordon field equation (2.12) for $m = 0$ becomes

$$\frac{1}{r^{d-2}} \partial_r (r^d A(r) \partial_r \Phi) - \frac{R^4}{r^2 A(r)} \partial_t^2 \Phi - \frac{R^2}{r^2} \nabla^2 \Phi = 0, \quad (2.28)$$

where

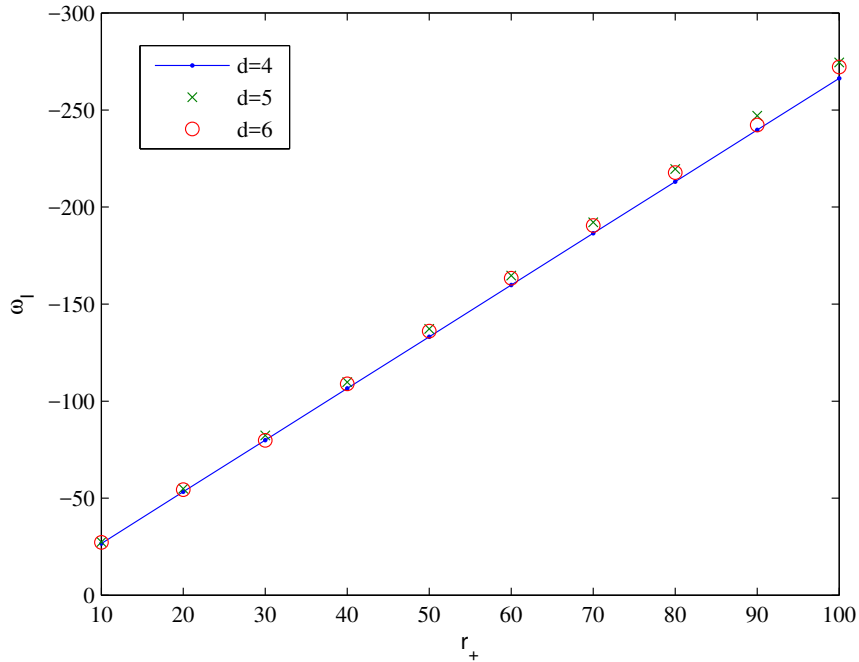


Figure 2.2: ω_I vs r_+ plot for large black holes in first order theories

$$A(r) = 1 - \left(\frac{r_h}{r}\right)^{\frac{d-1}{k}}. \quad (2.29)$$

We write the field Φ as

$$\Phi(t, r, x_i) = e^{i(\omega t - \vec{p} \cdot \vec{x})} \Psi(r), \quad (2.30)$$

and change the variable from r to

$$y = \left(\frac{r}{r_h}\right)^{\frac{d-1}{2k}}, \quad (2.31)$$

so that (2.28) becomes

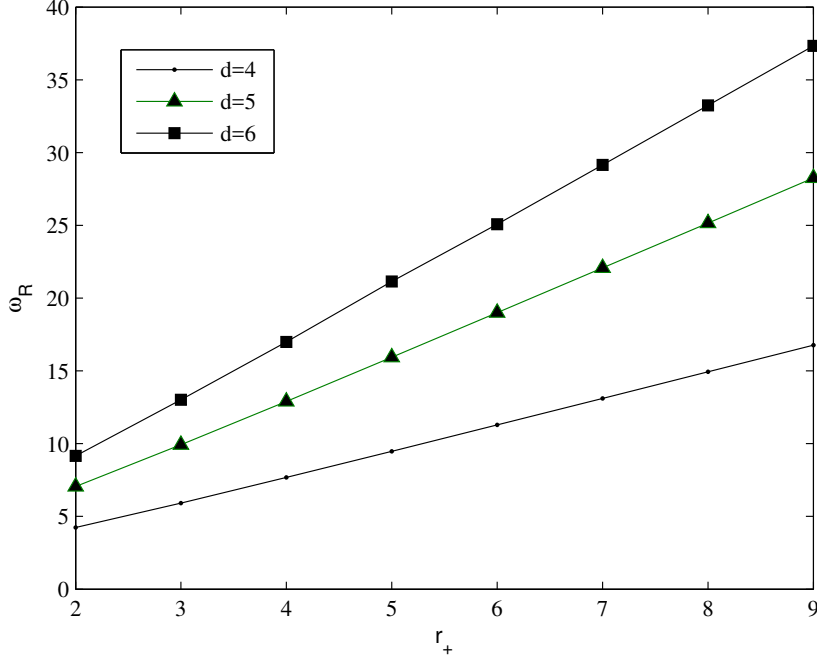


Figure 2.3: ω_R vs r_+ plot for intermediate black holes in first order theories

$$y^Q(y^2 - 1) (y^{2k-1}(y^2 - 1)\Psi')' + \left[\frac{\hat{\omega}^2}{A^2} y^2 - \frac{\hat{p}^2}{A^2} (y^2 - 1) \right] \Psi = 0, \quad (2.32)$$

where the parameters $\hat{\omega}$ and \hat{p} are defined as

$$\hat{\omega} = \frac{\omega R^2}{r_h}, \quad \hat{p} = \frac{|\vec{p}| R}{r_h}, \quad (2.33)$$

and

$$Q = \frac{6k - (2k - 1)d - 1}{d - 1}, \quad A = \frac{d - 1}{2k}. \quad (2.34)$$

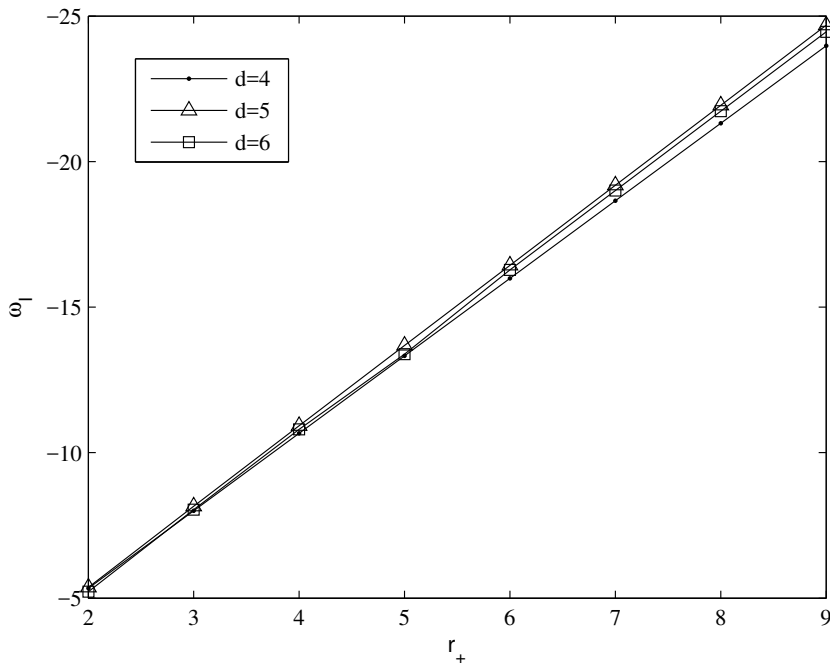


Figure 2.4: ω_I vs r_+ plot for intermediate black holes in first order theories

We investigate the behavior of (2.32) near the boundaries $y \rightarrow 1$ and $y \rightarrow \infty$ and the point $y \rightarrow -1$ in order to develop an ansatz for $\Psi(y)$. The following solutions are obtained:

$$\Psi \sim \begin{cases} y^{-2k} & , y \rightarrow \infty \\ (y-1)^{\pm i\hat{\omega}/2A} & , y \rightarrow 1 \\ (y+1)^{\pm \hat{\omega}/2A} & , y \rightarrow -1 \end{cases} \quad (2.35)$$

Since we demand ingoing plane wave like solutions at the horizon, we take the form $\Psi \sim (y-1)^{-i\hat{\omega}/2A}$ near the horizon ($y = 1$). We isolate the solutions near $y = \pm 1$ and write

$$\Psi(y) = (y-1)^{-i\hat{\omega}/2A} (y+1)^{\pm \hat{\omega}/2A} N(y). \quad (2.36)$$

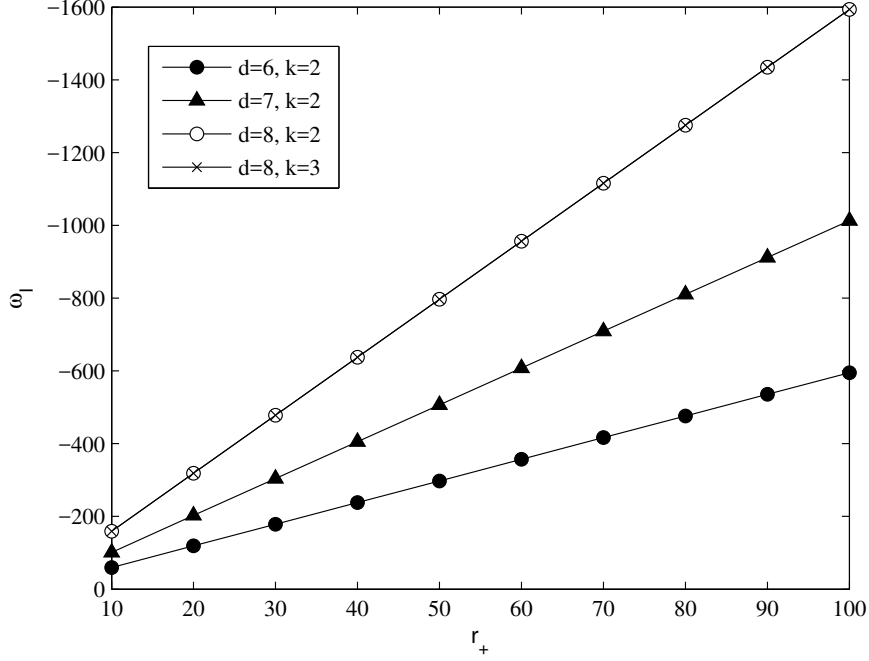


Figure 2.5: ω_I vs r_+ plot for large black holes in higher order theories

Substituting (2.36) in (2.32), we deduce the equation satisfied by $N(y)$ as

$$\begin{aligned}
 & y(y^2 - 1)N'' - \frac{\hat{\omega}^2 y^2}{A^2(y^2 - 1)}N + \\
 & + \left\{ \frac{\hat{\omega}}{A} \left(\mp \frac{i\hat{\omega}}{2A} \pm k - ik \right) y - (i \pm 1)(2k - 1) \frac{\hat{\omega}}{2A} \right\} N \\
 & \left\{ \left(2k + 1 - \frac{i \mp 1}{A} \hat{\omega} \right) y^2 - \frac{i \pm 1}{A} \hat{\omega} y - (2k - 1) \right\} N' \\
 & + \frac{1}{y^{Q+2k-2}} \left(\frac{\hat{\omega}^2 y^2}{A^2(y^2 - 1)} - \frac{\hat{p}^2}{A^2} \right) N = 0. \quad (2.37)
 \end{aligned}$$

We consider (2.37) in the range of large $\hat{\omega}$ and large y , so that $y^2 \approx y^2 - 1$ and the terms proportional to $1/(y^{Q+2k-2})$ may be dropped

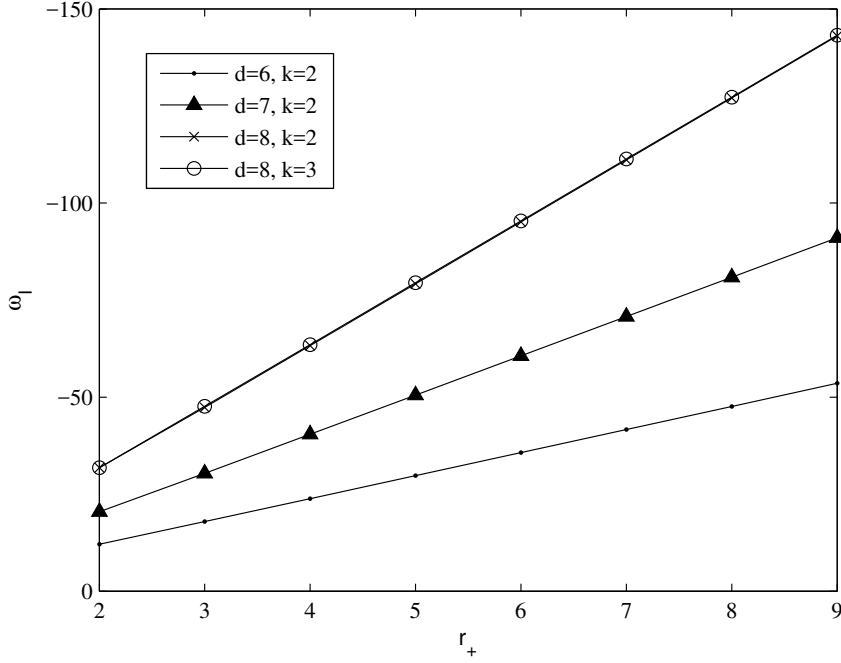


Figure 2.6: ω_I vs r_+ plot for intermediate black holes in first order theories

along with the constant terms. Then (2.37) reduces to

$$(y^2 - 1)N'' + \frac{\hat{\omega}}{A} \left(\mp \frac{i\hat{\omega}}{2A} \pm k - ik \right) N + \left\{ \left((2k + 1) - \frac{i \mp 1}{A} \hat{\omega} \right) y - \frac{i \pm 1}{A} \hat{\omega} \right\} N' = 0, \quad (2.38)$$

which is the Hypergeometric equation with the solution

$$N(y) = {}_2F_1(a, b; c; (y + 1)/2), \quad (2.39)$$

where

$$a = k - \frac{i \mp 1}{2A} \hat{\omega} + k, \quad b = -\frac{i \mp 1}{2A} \hat{\omega}, \quad c = \frac{2k + 1}{2} \pm \frac{\hat{\omega}}{A}. \quad (2.40)$$

In order to match the behavior of the solution (2.36) at infinity with that demanded by (2.35), we demand that $N(y)$ be a polynomial as $y \rightarrow \infty$. That condition is satisfied when

$$a = -n, \quad n = 1, 2, \dots \quad (2.41)$$

If $a = -n$, then, according to the property of the hypergeometric equation, $N(y) \sim y^n = y^{-a}$, so that, according to (2.36),

$$\begin{aligned} \Psi &\sim (y-1)^{-i\hat{\omega}/2A} (y+1)^{\pm\hat{\omega}/2A} y^{-a} \\ &\approx y^{-i\hat{\omega}/2A} y^{\pm\hat{\omega}/2A} y^{-a} = y^{-2k}, \end{aligned} \quad (2.42)$$

as required. We deduce the expression for the asymptotic form of quasi normal frequencies from (2.41) as follows:

$$\begin{aligned} a = -n &\Rightarrow 2k - \frac{i \mp 1}{2A} \hat{\omega} = -n \\ \Rightarrow \hat{\omega}_{asy} &= A(n + 2k)(\pm 1 - i), \end{aligned} \quad (2.43)$$

so that (2.33) implies

$$\omega_{asy} = A \left(\frac{r_h}{R^2} \right) (n + 2k)(\pm 1 - i), \quad (2.44)$$

which gives the asymptotic form of the quasi normal frequencies for large maximally symmetric AdS black holes in the Lovelock model. We observe that the high-overtone quasi normal frequencies are equispaced, which is in agreement with earlier observations [31, 34, 37].

2.4.1 Area Spectrum

We calculate the area spectrum of the large AdS black holes in Lovelock model using the new physical interpretation of the quasi normal

modes proposed by Maggiore [43] and following Kunstatter's method [52]. According to the first law of black hole thermodynamics, for a black hole system with energy E (or M) with Hawking temperature T_H and horizon area A , the following relation holds:

$$dM = \frac{1}{4}T_H dA. \quad (2.45)$$

According to Kunstatter, if the frequency of oscillation of the system is $\omega(E)$, then the quantity

$$I = \int \frac{dE}{\omega(E)}, \quad (2.46)$$

is to be taken as the corresponding adiabatic invariant. According to Maggiore [43], the black hole system has to be modeled by a collection of damped harmonic oscillators. If the system has a quasi normal frequency $\omega = \omega_R + i\omega_I$, then the corresponding vibrational frequency according to the model is to be taken as

$$\omega_0 = \sqrt{\omega_R^2 + \omega_I^2}. \quad (2.47)$$

In the highly damped and highly excited cases, ω_0 can be approximated by ω_I and ω_R respectively. Here, we see that for higher values of the number n , the both ω_R and ω_I increase. Therefore we consider transitions between two adjacent energy levels of the system and take the physical frequency as equal to the difference in ω_0 for the two systems; that is, we take

$$\omega(E) = \Delta\omega = (\omega_0)_n - (\omega_0)_{n-1}. \quad (2.48)$$

We deduce the area spectrum from (2.46) using the relations (2.27) and (2.44). The expression for the adiabatic invariant now reads

$$I = \int \frac{dE}{\omega(E)} = \int \frac{dM}{\Delta\omega} = \int \left(\frac{dM}{dr_h} \right) \left(\frac{1}{\Delta\omega} \right) dr_h. \quad (2.49)$$

Using (2.27), (2.44), (2.47) and (2.48) in (2.49), it is easy to see that the Bohr-Sommerfeld quantization condition, namely $I = n\hbar$ now reads

$$\left(\frac{d-1}{d-2} \right) \left(\frac{1}{2\sqrt{2}AG_k R^{2k-2}} \right) r_h^{d-2} = n\hbar, \quad (2.50)$$

which, in terms of the area \mathcal{A} of the horizon, can be written in the form

$$\mathcal{A} = \gamma n\hbar, \quad (2.51)$$

where

$$\gamma = \left[\Gamma \left(\frac{d-1}{2} \right) \left(\frac{d-1}{d-2} \right) \left(\frac{1}{4\sqrt{2}\pi^{(d-1)/2} AG_k R^{2k-2}} \right) \right]^{-1}. \quad (2.52)$$

Thus the area spectrum, and consequently the entropy spectrum, of large black holes in asymptotically AdS Lovelock spacetimes is seen to depend on the parameters G_k and the AdS radius R of the theory. The dependence of \mathcal{A} on R is observed only when higher orders are considered. \mathcal{A} is also dependent on the dimension d of the spacetime, and consequently on the order of the theory.

2.5 Conclusion

We have analyzed the evolution of massless Klein-Gordon field in the maximally symmetric asymptotically AdS spacetime surrounding a black hole in the Lovelock model. We have used the form of the metric

that has been derived in [50] in order to compute the quasi normal frequencies using the Horowitz-Hubeny method. The results of the numerical computation show that the modes in the case of higher order theories are purely damped. For the case of large as well as intermediate black holes, the frequencies are observed to scale linearly with the temperature of the event horizon. When we consider higher order theories, the imaginary part of the quasi normal frequencies is observed to be independent of the order of the theory in higher dimensions. They appear to be dependent on the dimension only.

The asymptotic form of the quasi normal frequencies for the case of very large black holes has been analytically determined using the method of perturbative expansion of the wave equation in terms of ω/T_H , as developed in [51]. We find that the asymptotic modes are equispaced, in agreement with previous results. We have also calculated the area spectrum spacing and found it to be dependent on the value of R , d and k . This is also in contrast to the case of first order theories where we always obtain area spectra that are equidistant even when the parameters of the black hole spacetime change.

3

Quasinormal Modes of Lovelock Black Holes

3.1 Introduction

In the previous chapter, we studied the Quasinormal modes (QNMs) of Lovelock black holes in asymptotically AdS spacetimes. In this chapter, we focus our attention on asymptotically flat black hole solutions. As mentioned in Chapter 1, the long-lived modes in asymptotically flat spacetimes surrounding black holes are expected to be observed in the future by gravitational wave detectors. Different models of gravity predict different “quasinormal signatures” of their respective spacetimes and the experimental observation of these modes may well put to rest the problem of selecting the most suitable model for gravity from existing (numerous) ones.

The research on QNMs is decades old with an extensive literature (for example, [31–36, 57–61] and references therein). The quasinormal behavior in first order theories of gravity such as the General Theory of Relativity (GTR) is particularly well studied with its asymptotic behavior firmly established both numerically and analytically [62]. The asymptotic quasinormal modes of perturbations in GTR have their real parts approach a constant value, while the imaginary parts

increase indefinitely. These modes are significant from the standpoint of quantum theories of gravity since they help us to compute the area spectrum and subsequently the entropy of the black hole event horizons, which, in GTR, are known to be equally spaced. The asymptotic behavior of the modes, observed numerically, can help one analytically determine the precise form of these modes in terms of the parameters of the theory later. This has been demonstrated in [62], where the decision to compute the monodromy along the Stokes line was made because of the asymptotic behavior mentioned above. Thus it would be highly interesting to see how the quasinormal modes behave asymptotically in any model of gravity that one considers.

The connection between geodesic stability and quasinormal modes in black hole spacetimes has been known for a long time ([32, 33, 63, 64, 66]). These studies reveal the connection between quasinormal modes of black hole spacetimes and the dynamics of null particles in an unstable circular orbit around the black hole, with its energy slowly leaking out. The relation is most clearly established in [63] for any static, spherically symmetric and asymptotically flat spacetime, according to which the quasinormal frequencies ω_{asy} in the limit ($l \rightarrow \infty$) is given by

$$\omega_{asy} = \Omega_c l - i(n + \frac{1}{2})|\lambda|, \quad (3.1)$$

where Ω_c and λ are the angular velocity at the unstable null geodesic and the principal Lyapunov exponent which is related to the time scale of energy decay in the orbit.

The actual number of spacetime dimensions is predicted to be higher than four by string theory and it has led to attempts at de-

veloping models of gravity in higher dimensions. In these higher dimensional spacetimes, GTR no longer is the most general model of gravity. Generalizations of GTR are naturally attempted by adding higher order curvature correction terms to the Einstein-Hilbert action. Among such generalizations to GTR, the Lovelock model [14, 145], considered as a natural generalization of the GTR to higher dimensions and orders of curvature, is particularly interesting since it yields field equations of second order that are free of ghosts. The Lovelock Lagrangian consists of dimensionally continued curvature terms of orders one and above. The resulting theories are labeled by the order of the maximum-ordered term, k , which in turn is determined by the dimension of the spacetime d , by $k = \lfloor \frac{d-1}{2} \rfloor$ where $\lfloor x \rfloor$ denotes the integer part of x . Black hole solutions to the theory in general contain many branches that depend on the values of the higher order coupling constants [16]. It is known [19] that the metric perturbations to the most general, asymptotically flat Lovelock spacetime are unstable in the ultraviolet region. Therefore it is necessary to impose further constraints to select a suitable set of Lovelock theories which would permit stable perturbations. Such maximally symmetric, asymptotically flat as well as AdS spacetimes have been known for a long time [50].

In this chapter, we compute the quasinormal modes of metric perturbations to the metric of such maximally symmetric spacetimes using the sixth order WKB method [71]. We analytically determine the asymptotic form of these modes using the above-mentioned null geodesic method. The chapter is organized as follows: in Sect. 3.2, we describe the essential details of the null geodesic method used to compute the asymptotic form of the modes. In Sect. 3.2.1, we describe

the class of Lovelock theories for which the modes are computed and the WKB expression of numerical computation. The relation between the asymptotic quasinormal modes and the null geodesic parameters is expressed in Sect. 3.2.2. The results of the calculation are discussed in Sect. 3.3. We summarize the main results in Sect. 3.4.

3.2 Geodesic Stability

Consider the general stationary and spherically symmetric metric

$$ds^2 = f(r)dt^2 - \frac{1}{g(r)}dr^2 - r^2d\Omega_{d-2}^2, \quad (3.2)$$

where $f(r)$ and $g(r)$ are solutions of the Lovelock field equations [16]. $d\Omega_{d-2}^2$ represents the metric of the spherically symmetric background. For this metric, we have the Lagrangian in the form,[70]

$$2\mathcal{L} = f(r)\dot{t}^2 - \frac{1}{g(r)}\dot{r}^2 - r^2\dot{\varphi}^2, \quad (3.3)$$

where a dot represents derivative with respect to proper time and φ is an angular coordinate. For this system, the coordinate angular velocity Ω_c and the principal Lyapunov exponent λ for circular null geodesics take the form, [63]

$$\Omega_c = \frac{\dot{\varphi}}{\dot{t}} = \left(\frac{f'_c}{2r_c} \right)^{1/2}, \quad (3.4)$$

$$\lambda = \frac{1}{\sqrt{2}} \sqrt{-\frac{r_c^2}{f_c} \left(\frac{d^2 f}{dr_*^2 r^2} \right)_{r=r_c}}, \quad (3.5)$$

where the subscript c means that the evaluation is done at the critical radius, $r = r_c$, which satisfies the relation $2f - rf' = 0$. r_c can be viewed as the innermost circular timelike geodesic, since circular

timelike geodesics satisfy $2f - rf' > 0$. r_* is the tortoise coordinate which satisfies the relation $dr_* = \frac{dr}{\sqrt{g(r)f(r)}}$.

3.2.1 The Equations of Perturbation and the WKB Method

The action I_G for the class of Lovelock theories, a subset of which are studied in this work, is written as [14, 50, 53],

$$I_G = \kappa \int \sum_{p=0}^k \alpha_p L^{(p)}, \quad (3.6)$$

where α_p are positive coupling constants and $L^{(p)}$, given by

$$L^{(p)} = \epsilon_{a_1 \dots a_d} R^{a_1 a_2} \dots R^{a_{2p-1} a_{2p}} e^{a_{2p+1}} \dots e^{a_d}, \quad (3.7)$$

are the p^{th} order dimensionally continued terms in the Lagrangian, $\epsilon_{a_1 \dots a_d}$ being the Levi-Civita symbol. κ is a parameter related to the gravitational constant G_k by $\kappa = \frac{1}{2(d-2)! \Omega_{d-2} G_k}$, Ω_{d-2} being the volume of the $(d-2)$ dimensional spherically symmetric tangent space with unit curvature. R^{ab} represents the Riemann curvature and e^a represents the vielbein.

The resulting field equations are of the form

$$\epsilon_{ba_1 \dots a_{d-1}} \bar{R}^{a_1 a_2} \dots \bar{R}^{a_{2k-1} a_{2k}} e^{a_{2k+1}} \dots e^{a_{d-1}} = 0 \quad (3.8)$$

$$\epsilon_{aba_3 \dots a_d} \bar{R}^{a_3 a_4} \dots \bar{R}^{a_{2k-1} a_{2k}} T^{a_{2k+1}} e^{a_{2k+2}} \dots e^{a_{d-1}} = 0 \quad (3.9)$$

Here, $\bar{R}^{ab} := R^{ab} + \frac{1}{R^2} e^a e^b$.

It is known [19] that the theories in which all the higher order coupling constants α_p are positive permit asymptotically flat space-time solutions that suffer from dynamical instability against metric perturbations. In the present chapter, we consider a special case. We consider the class of theories with α_p given by

$$\alpha_p = \frac{1}{d-2k} \delta_p^k. \quad (3.10)$$

The static and spherically symmetric black hole solutions of the theory, written in Schwarzschild-like coordinates, take the form

$$ds^2 = f(r)dt^2 + \frac{dr^2}{f(r)} + r^2 d\Omega_{d-2}^2, \quad (3.11)$$

where $f(r)$ is given by

$$f(r) = 1 - \left(\frac{2G_k M}{r^{d-2k-1}} \right)^{1/k}, \quad (3.12)$$

M being the mass of the black hole. It is to be noted that only the cases in which $d-2k-1 \neq 0$ yield black hole solutions [50] with their event horizons r_h located at $(2G_k M)^{\frac{1}{d-2k-1}}$. It is noted that for the case of $d=4$ and $k=1$, we get the Schwarzschild geometry of GTR. We can therefore consider these spacetimes as natural generalizations of the former to the case of higher order theories in higher dimensions. The master equations obeyed by the metric perturbations for the general Lovelock theory were derived in [16].

The master equation satisfied by the tensor metric perturbation $\delta g_{ij} = r^2 \phi(t, r) h_{ij}(x^i)$, after separating the variables $\phi(r, t) = \chi(r) e^{-i\omega t}$, takes the form [16],

$$-f^2 \chi'' - \left(f^2 \frac{T''}{T'} + \frac{2f^2}{r} + f f' \right) \chi' + \frac{(2\kappa + \gamma_t) f T''}{(n-2)r T'} \chi = \omega^2 \chi, \quad (3.13)$$

where the function $T(r)$, for the most general class of Lovelock theories given by (3.6) with all the constants α_p being positive, is given by the expression

$$T(r) = r^{n-1} \left(1 + \sum_{m=2}^k \left[a_m \left\{ \prod_{p=1}^{2m-2} (n-p) \right\} \psi^{m-1} \right] \right), \quad (3.14)$$

where $\psi(r)$ is defined by the relation $f(r) = 1 - r^2\psi(r)$. We write $\Psi(r) = \chi(r)r\sqrt{T'(r)}$ and define the tortoise coordinate r^* by $dr^* = dr/f(r)$ to transform (3.13) to the form

$$\frac{d^2\Psi}{dr^{*2}} + (\Omega^2 - V(r))\Psi = 0, \quad (3.15)$$

Here, $V(r) = V_t(r)$, the effective potential for tensor perturbations. The tortoise coordinate r^* is defined by $dr^* = dr/f(r)$. Similar expressions for the vector and scalar type perturbations can be derived easily. The effective potentials $V(r)$ for tensor ($V_t(r)$), vector ($V_v(r)$) and scalar ($V_s(r)$) perturbations are given below:

$$V(r) = \begin{cases} V_t(r) = \frac{(2\kappa+\gamma_t)f}{(n-2)r} \frac{d \ln T'}{dr} + \frac{1}{r\sqrt{T'}} f \frac{d}{dr} \left(f \frac{d}{dr} r \sqrt{T'} \right) \\ V_v(r) = r\sqrt{T'} f \partial_r \left(f \partial_r \frac{1}{r\sqrt{T'}} \right) + \frac{f}{r} \left(\frac{\gamma_v}{n-1} - \kappa \right) \frac{T'}{T} \\ V_s(r) = 2\gamma_s f \frac{(rNT)'}{nr^2NT} - f \left(\frac{1}{N} \partial_r (f \partial_r N) + \frac{1}{T} \partial_r (f \partial_r T) \right) \\ + 2f^2 \left(\frac{N'^2}{N^2} + \frac{T'^2}{T^2} + \frac{N'T'}{NT} \right) \end{cases} \quad (3.16)$$

Here, $\gamma_t = l(l+d-3)-2$, $\gamma_v = l(l+d-3)-1$ and $\gamma_s = l(l+d-3)$ are the eigenvalues for the tensor, vector and scalar harmonics respectively.

The functions $T(r)$ and $N(r)$, for the class of theories given by (3.10), are given by

$$T(r) = \left(\prod_{p=1}^{2k-2} (d-p-2) \right) \left(\frac{2G_k M}{r^{d-1}} \right)^{1-\frac{1}{k}},$$

$$N(r) = \frac{2\gamma_s - 2(d-2)f + (d-2)rf'}{r\sqrt{T'}}. \quad (3.17)$$

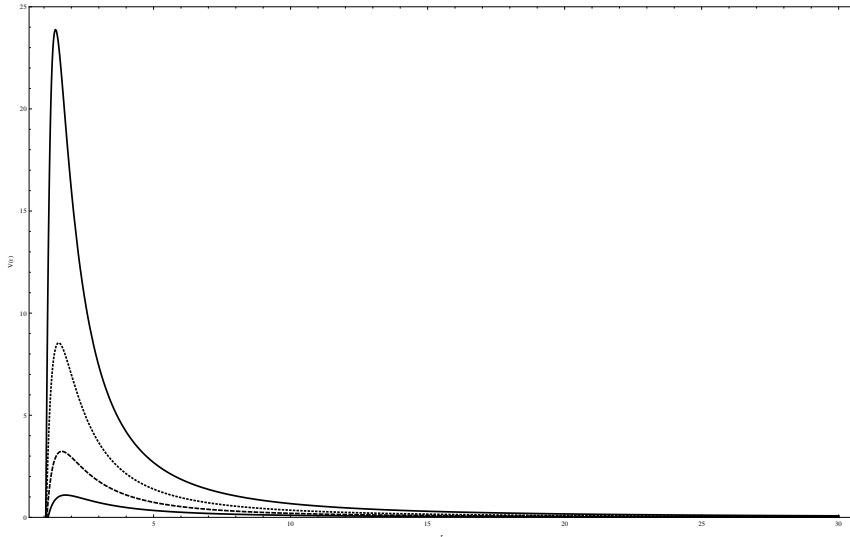


Figure 3.1: Effective potential $V(r)$ vs r for different k , from $k = 2$ (top) to $k = 5$ (bottom), with $d = 17$ and $l = 7$.

Fig. 3.1 represents the typical variation of the effective potential $V(r)$ outside the event horizon for all types of perturbations. The different plots are drawn for different values of k which is the tunable parameter for the set of theories studied in this work. It is noted that the potential is barrier-like for all values of k . The height of the barrier is seen to be a decreasing function of the order parameter k .

We now apply the WKB method in order to compute the QNMs of the metric perturbations that obey (3.15). The third order WKB formula for QNMs was derived by Iyer and Will [60] and was extended to the sixth order by Konoplya [71]. We use the sixth order formula derived in [71] since it gives better accuracy for lower modes.

The sixth order formula for computing the QNM Ω for perturbations obeying (3.15) is given by

$$\frac{Q_0}{\sqrt{2Q_0''}} - \Lambda_2 - \Lambda_3 - \Lambda_4 - \Lambda_5 - \Lambda_6 = i \left(n + \frac{1}{2} \right), \quad (3.18)$$

where n is the overtone number and we have used the notation $Q(x) = \Omega^2 - V(x)$. $Q_0 = Q(x_0)$, where x_0 is the tortoise coordinate at which the potential attains its peak. Also, prime (') represents differentiation with respect to the tortoise coordinate x . The expressions for the correction terms $\Lambda_2, \Lambda_3, \Lambda_4, \Lambda_5$ and Λ_6 are given in [71] and [72].

3.2.2 Asymptotic Quasinormal Modes in terms of Null Geodesic Parameters

In order to find an approximate analytic expression for the quasinormal modes in the asymptotic limit $l \rightarrow \infty$, we drop the higher order terms in (3.18) and write

$$\frac{Q_0}{\sqrt{2Q_0''}} = i \left(n + \frac{1}{2} \right). \quad (3.19)$$

It can be seen that in the limit $l \rightarrow \infty$, the effective potentials $V(r)$ for all three types of perturbations, given by (3.16), reduce to much simpler forms so that simple expressions are obtained for the corresponding functions Q_0 as follows:

$$Q_0 \simeq \Omega^2 - Cl^2 \frac{f}{r^2}, \quad (3.20)$$

where the values of the parameter C for tensor (C_t), vector (C_v) and scalar (C_s) perturbations in d dimensions for the Lovelock theory of order k take the form:

$$C = \begin{cases} C_t = \frac{1}{d-4} \left[(d-4) - (k-1) \left(\frac{d-1}{k} \right) \right] \\ C_v = \frac{1}{d-3} \left[(d-3) - (k-1) \left(\frac{d-1}{k} \right) \right] \\ C_s = \frac{1}{d-2} \left[(d-2) - (k-1) \left(\frac{d-1}{k} \right) \right] \end{cases} \quad (3.21)$$

Substituting (3.21) and (3.20) into (3.19), we get the following expression for the quasinormal modes in the limit $l \rightarrow \infty$:

$$\Omega_{asy} = l\sqrt{C} \sqrt{\frac{f_c}{r_c^2}} - i \frac{(n + \frac{1}{2})}{\sqrt{2}} \sqrt{-\frac{r_c^2}{f_c} \left[\frac{d^2}{dr_*^2} \left(\frac{f}{r^2} \right) \right]_{r=r_c}}, \quad (3.22)$$

with C taking appropriate values depending on the type of perturbation under consideration. The connection between Ω_{asy} and the null geodesic parameters is clear from (3.4), (3.5) and (3.22). Clearly, the real parts of the modes vary linearly with l while the imaginary parts are independent of l . Thus, for the same value of n , the imaginary parts of the modes should approach a constant. Also, given sufficiently high value of the parameter d , we have $C_t \simeq C_v \simeq C_s$,

which means that the metric perturbations of the spacetime given by (3.11) should be isospectral if one considers Lovelock theories given by (3.6) in very high dimensions.

3.3 Results and Discussion

We use (3.18) to compute the QNMs Ω for various combinations of spacetime dimension d and the order parameter k . The calculation is done for different values of the mode number n . We have tabulated the low-lying modes for $l = 2$ in Tables 3.1, 3.2 and 3.3. The parameter l is given values from 6 to 80 and selected values of the QNMs are tabulated in tables 3.4, 3.5 and 3.6. In Table 3.7, we compare the values of QNMs obtained using the eikonal approximation and the sixth order WKB method, for tensor and vector perturbations. The corresponding comparison for scalar perturbations is summarized in Table 3.8. Tables 3.9, 3.10 and 3.11 show the QNMs for various values of the order k . In all tables and figures in this work, ω stands for $\Omega G_k M$, where Ω is the QNM calculated using (3.18).

As far as figures are concerned, we have chosen to include the relevant figures obtained from the numerical data only for the case of tensor perturbations. The justification for doing so is twofold - it saves space and, more importantly, it helps us avoid redundancy, since the behavior of the QNFs depicted in those figures is mimicked in the corresponding figures for the other two types of perturbations - vector and scalar.

Fig. 3.2 is the $\log - \log$ plot of the real and imaginary parts of the QNFs for tensor modes, which show their behavior as the parameter

l varies from relatively low values to high values. From the plot, we observe a behavior that is consistent with that suggested by the null geodesic method. We see that the the imaginary parts of the modes tend to become a constant at high values of l , as seen in (3.22). The behavior of the imaginary parts for lower values of l is similar to that in an earlier work [73] which also shows a convergent pattern for $\text{Im } \omega$ as l increases.

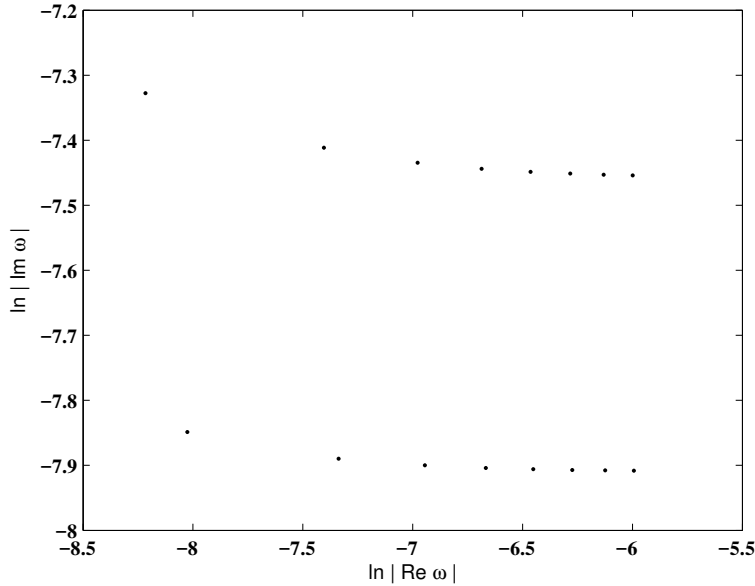


Figure 3.2: Tensor modes for $k = 2$ and $d = 8$, for $n = 5$ (top) and $n = 3$ (bottom). The plotted points within each curve are for $l = 10$ (left) to $l = 80$ (right).

Fig. 3.3 shows the variation of the the logarithm of the the absolute values of the real parts of the tensor QNFs with spacetime dimension d . As observed from the plot, the real parts decrease as d increases, indicating modes with lower frequency in higher dimensions. For any

value of d , the real parts increase with increasing values of l .

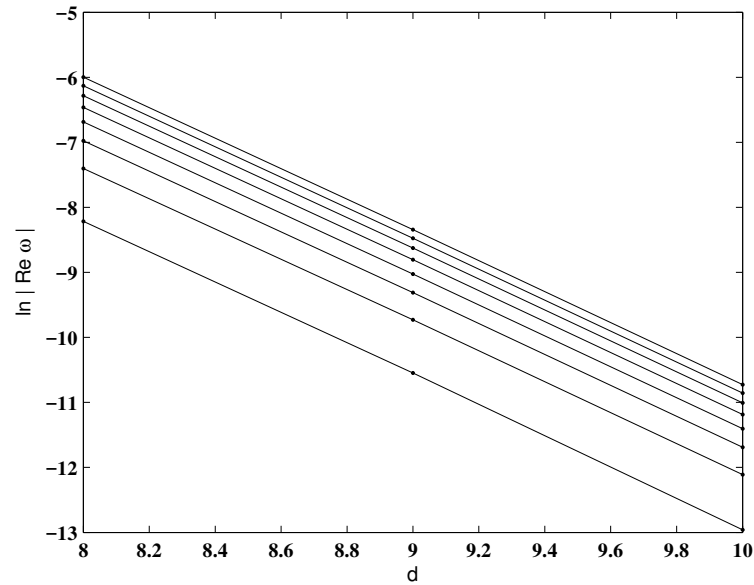


Figure 3.3: Variation of $\ln |Re(\omega)|$ vs d for $k = 2$ for Tensor modes . Here, $n = 5$. The curves are for $l = 10$ (bottom) to $l = 50$ (top).

Figs. 3.4 and 3.5 show the variation of the logarithm of the the absolute values of the real and imaginary parts of the tensor QNFs with the order parameter k . As observed from the plots, the real parts as well as the imaginary parts increase as k increases.

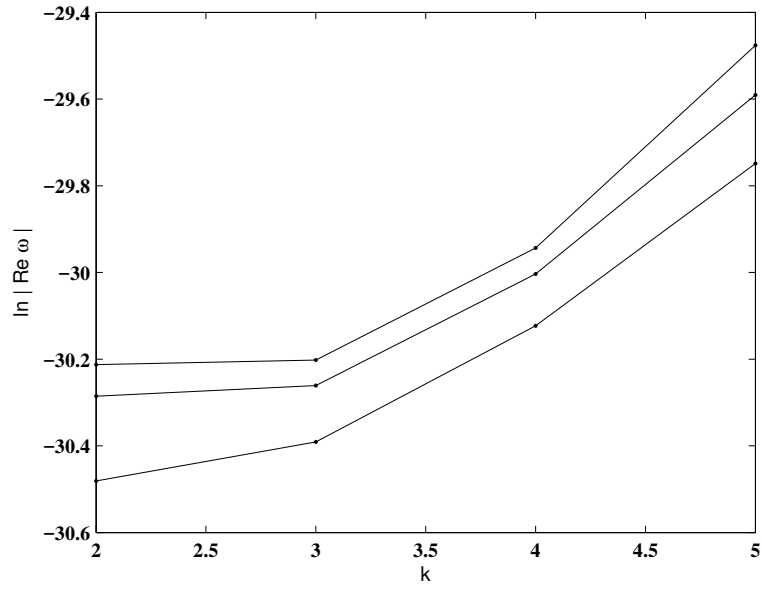


Figure 3.4: Variation of $\ln |Re(\omega)|$ vs k for $d = 17$ and $l = 7$ for Tensor modes . The curves are for $n = 0$ (top) to $n = 2$ (bottom).

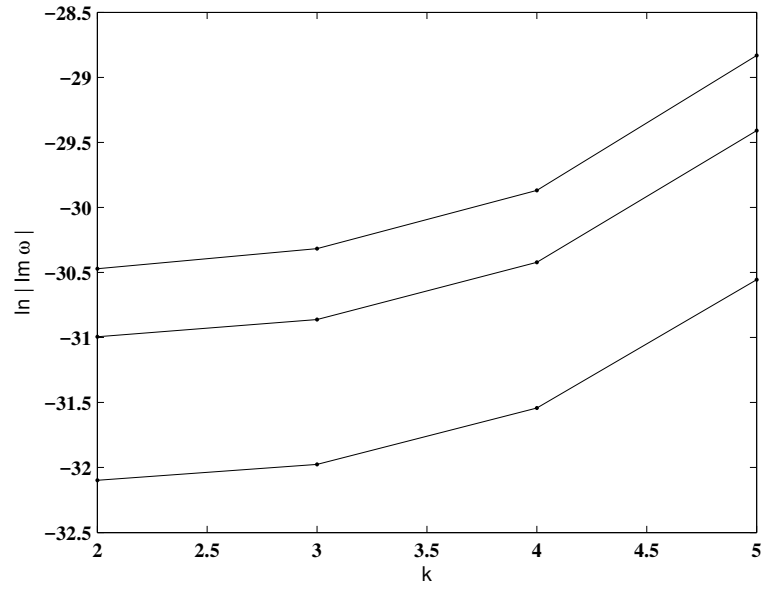


Figure 3.5: Variation of $\ln |Im(\omega)|$ vs k for $d = 17$ and $l = 7$ for Tensor modes . The curves are for $n = 0$ (bottom) to $n = 2$ (top).

Table 3.1: Low-lying modes for Tensor perturbations for various dimensions (in units of 10^{-6})

l	n	ω ($d = 8, k = 2$)	ω ($d = 9, k = 2$)	ω ($d = 10, k = 2$)
2	0	133.1406 - 54.2445 <i>i</i>	13.4214 - 4.7089 <i>i</i>	1.3217 - 0.4333 <i>i</i>
2	1	112.3407 - 173.8648 <i>i</i>	11.3954 - 15.0050 <i>i</i>	1.1125 - 1.3804 <i>i</i>
2	2	91.9167 - 316.0219 <i>i</i>	8.5470 - 27.6200 <i>i</i>	0.7721 - 2.5675 <i>i</i>
3	0	164.0819 - 53.5968 <i>i</i>	16.4993 - 4.6478 <i>i</i>	1.6117 - 0.4271 <i>i</i>
3	1	145.2940 - 168.7927 <i>i</i>	14.7436 - 14.5361 <i>i</i>	1.4336 - 1.3333 <i>i</i>
3	2	120.0297 - 303.0023 <i>i</i>	11.8915 - 26.0985 <i>i</i>	1.1173 - 2.4025 <i>i</i>
3	3	103.2647 - 458.7079 <i>i</i>	8.8570 - 40.1800 <i>i</i>	0.7309 - 3.7512 <i>i</i>
4	0	194.8473 - 53.2421 <i>i</i>	19.5138 - 4.6210 <i>i</i>	1.8935 - 0.4247 <i>i</i>
4	1	178.1521 - 165.5511 <i>i</i>	17.9892 - 14.2800 <i>i</i>	1.7400 - 1.3099 <i>i</i>
4	2	152.4328 - 292.9591 <i>i</i>	15.3267 - 25.1695 <i>i</i>	1.4547 - 2.3105 <i>i</i>
4	3	128.2170 - 439.3342 <i>i</i>	12.1695 - 37.9506 <i>i</i>	1.0840 - 3.5106 <i>i</i>
4	4	114.7935 - 606.6123 <i>i</i>	9.1155 - 53.2629 <i>i</i>	0.6793 - 4.9998 <i>i</i>

Table 3.2: Low-lying modes for Vector perturbations for various dimensions (in units of 10^{-6})

l	n	ω ($d = 7, k = 2$)	ω ($d = 8, k = 2$)	ω ($d = 9, k = 2$)	ω ($d = 10, k = 2$)
2	0	1987.1950 - 730.1241 <i>i</i>	134.2193 - 50.3052 <i>i</i>	11.9857 - 4.4229 <i>i</i>	-
2	1	1608.5488 - 2369.9620 <i>i</i>	108.6194 - 161.0435 <i>i</i>	9.5496 - 14.0856 <i>i</i>	-
2	2	1060.5751 - 4440.9963 <i>i</i>	66.9691 - 302.4766 <i>i</i>	5.2406 - 26.7137 <i>i</i>	-
3	0	3062.5553 - 728.6387 <i>i</i>	196.1230 - 48.6493 <i>i</i>	16.7160 - 4.2920 <i>i</i>	1.5269 - 0.4004 <i>i</i>
3	1	2838.5908 - 2241.7117 <i>i</i>	176.6061 - 150.7660 <i>i</i>	14.6955 - 13.4016 <i>i</i>	1.3218 - 1.2518 <i>i</i>
3	2	2446.9666 - 3914.5570 <i>i</i>	141.2707 - 267.9013 <i>i</i>	11.0103 - 24.1834 <i>i</i>	0.9361 - 2.2729 <i>i</i>
3	3	1981.3414 - 5816.5456 <i>i</i>	97.0424 - 409.3032 <i>i</i>	6.3318 - 37.7686 <i>i</i>	0.4302 - 3.5975 <i>i</i>
4	0	4014.3270 - 748.3938 <i>i</i>	253.8493 - 49.5175 <i>i</i>	21.3443 - 4.3038 <i>i</i>	1.9199 - 0.3974 <i>i</i>
4	1	3846.5184 - 2282.0116 <i>i</i>	239.8692 - 151.2782 <i>i</i>	19.8584 - 13.1766 <i>i</i>	1.7586 - 1.2201 <i>i</i>
4	2	3544.7474 - 3920.3525 <i>i</i>	213.8152 - 261.3232 <i>i</i>	16.9958 - 22.9209 <i>i</i>	1.4407 - 2.1399 <i>i</i>
4	3	3169.0262 - 5709.3996 <i>i</i>	179.5279 - 384.6027 <i>i</i>	13.0678 - 34.2095 <i>i</i>	0.9950 - 3.2436 <i>i</i>
4	4	2783.4865 - 7671.34073 <i>i</i>	141.2937 - 525.2555 <i>i</i>	8.4835 - 47.7143 <i>i</i>	0.4665 - 4.6197 <i>i</i>

Table 3.3: Low-lying modes for Scalar perturbations for various dimensions (in units of 10^{-6})

l	n	ω ($d = 7, k = 2$)	ω ($d = 8, k = 2$)	ω ($d = 9, k = 2$)	ω ($d = 10, k = 2$)
2	0	2547.5661 - 716.4415 <i>i</i>	205.36410 - 9.6575 <i>i</i>	-	2.3027 - 0.3208 <i>i</i>
2	1	2271.1626 - 2240.5828 <i>i</i>	334.0324 - 6.4720 <i>i</i>	-	6.9142 - 0.4909 <i>i</i>
2	2	1810.0458 - 3995.1437 <i>i</i>	90.0530 - 763.3169 <i>i</i>	-	15.6242 - 0.5226 <i>i</i>
3	0	3905.5647 - 746.6365 <i>i</i>	218.9954 - 46.7773 <i>i</i>	16.9439 - 3.9805 <i>i</i>	1.5315 - 0.2688 <i>i</i>
3	1	3733.1930 - 2278.6463 <i>i</i>	204.5237 - 142.9336 <i>i</i>	14.9968 - 13.7331 <i>i</i>	1.9261 - 0.4939 <i>i</i>
3	2	3424.6745 - 3920.6131 <i>i</i>	177.8404 - 246.4931 <i>i</i>	12.4106 - 29.1985 <i>i</i>	3.5782 - 0.1568 <i>i</i>
3	3	3043.6602 - 5720.0577 <i>i</i>	142.4973 - 361.3841 <i>i</i>	10.8457 - 52.7568 <i>i</i>	-
4	0	5111.2845 - 761.7854 <i>i</i>	290.4033 - 48.9992 <i>i</i>	22.7621 - 4.1094 <i>i</i>	1.9517 - 0.3631 <i>i</i>
4	1	4978.7417 - 2309.6889 <i>i</i>	278.8390 - 149.1029 <i>i</i>	21.5711 - 12.5907 <i>i</i>	1.8526 - 1.1095 <i>i</i>
4	2	4732.6146 - 3927.8632 <i>i</i>	257.1089 - 255.5290 <i>i</i>	19.3001 - 21.9070 <i>i</i>	1.6680 - 1.9276 <i>i</i>
4	3	4408.8671 - 5651.5157 <i>i</i>	228.0448 - 372.0127 <i>i</i>	16.2394 - 32.6401 <i>i</i>	1.4339 - 2.8909 <i>i</i>
4	4	4051.0515 - 7500.0861 <i>i</i>	195.0275 - 501.4720 <i>i</i>	12.7435 - 45.3070 <i>i</i>	1.2037 - 4.0923 <i>i</i>

Table 3.4: QNMs of Tensor perturbations for $n = 1$ (in units of 10^{-6})

l	ω ($d = 8, k = 2$)	ω ($d = 9, k = 2$)	ω ($d = 10, k = 2$)
10	368.5710 - 159.6868 <i>i</i>	36.3453 - 13.8559 <i>i</i>	3.4472 - 1.2732 <i>i</i>
20	676.4250 - 158.2275 <i>i</i>	65.7576 - 13.7504 <i>i</i>	6.1611 - 1.2638 <i>i</i>
30	981.4976 - 157.8903 <i>i</i>	94.8519 - 13.7256 <i>i</i>	8.8397 - 1.2616 <i>i</i>
40	1285.7250 - 157.7616 <i>i</i>	123.8498 - 13.7161 <i>i</i>	11.5075 - 1.2607 <i>i</i>
50	1589.5868 - 157.6991 <i>i</i>	152.8060 - 13.7114 <i>i</i>	14.1705 - 1.2603 <i>i</i>
60	1893.2578 - 157.6642 <i>i</i>	181.7402 - 13.7088 <i>i</i>	16.8310 - 1.2600 <i>i</i>
70	2196.8167 - 157.6427 <i>i</i>	210.6616 - 13.7071 <i>i</i>	19.4901 - 1.2599 <i>i</i>

Table 3.5: QNMs of Vector perturbations for $n = 1$ (in units of 10^{-6})

l	ω ($d = 8, k = 2$)	ω ($d = 9, k = 2$)	ω ($d = 10, k = 2$)
10	554.9965 - 155.8556 <i>i</i>	45.3264 - 13.5203 <i>i</i>	3.9634 - 1.2402 <i>i</i>
20	1039.3543 - 157.05278 <i>i</i>	84.0122 - 13.6437 <i>i</i>	7.2757 - 1.2529 <i>i</i>
30	1514.6547 - 157.0527 <i>i</i>	121.8428 - 13.6738 <i>i</i>	10.5038 - 1.2562 <i>i</i>
40	1987.3587 - 157.4331 <i>i</i>	159.4219 - 13.6856 <i>i</i>	13.7066 - 1.2575 <i>i</i>
50	2458.9581 - 157.4840 <i>i</i>	196.8927 - 13.6913 <i>i</i>	16.8984 - 1.2582 <i>i</i>
60	2929.9849 - 157.5124 <i>i</i>	234.3070 - 13.6946 <i>i</i>	20.0845 - 1.2585 <i>i</i>
70	3400.6768 - 157.5299 <i>i</i>	271.6881 - 13.6966 <i>i</i>	23.2670 - 1.2588 <i>i</i>

Table 3.6: QNMs of Scalar perturbations for $n = 1$ (in units of 10^{-6})

l	ω ($d = 8, k = 2$)	ω ($d = 9, k = 2$)	ω ($d = 10, k = 2$)
10	652.8312 - 155.8358 <i>i</i>	50.9723 - 13.4597 <i>i</i>	4.3254 - 1.2285 <i>i</i>
20	1224.3284 - 157.0746 <i>i</i>	95.0437 - 13.6313 <i>i</i>	8.0203 - 1.2502 <i>i</i>
30	1784.6681 - 157.3415 <i>i</i>	138.0091 - 13.6685 <i>i</i>	11.6034 - 1.2549 <i>i</i>
40	2341.8477 - 157.4900 <i>i</i>	180.6552 - 13.6826 <i>i</i>	15.1536 - 1.2568 <i>i</i>
50	2897.6879 - 157.4900 <i>i</i>	223.1647 - 13.6894 <i>i</i>	18.6895 - 1.2577 <i>i</i>
60	3452.8349 - 157.5165 <i>i</i>	265.6032 - 13.6932 <i>i</i>	22.2179 - 1.2582 <i>i</i>
70	4007.5767 - 157.5330 <i>i</i>	307.9999 - 13.6956 <i>i</i>	25.7420 - 1.2585 <i>i</i>

Table 3.7: Comparison between the eikonal approx. and the numerical values of tensor and vector QNMs ($d = 10$, $k = 2$ and $n = 1$) (in units of 10^{-6})

Tensor		Vector	
l	ω_{eik}	ω_{num}	ω_{num}
10	2.65511 - 1.34949 <i>i</i>	3.4472 - 1.2732 <i>i</i>	3.17346 - 1.34949 <i>i</i>
20	5.31022 - 1.34949 <i>i</i>	6.1611 - 1.2638 <i>i</i>	6.34692 - 1.34949 <i>i</i>
30	7.96532 - 1.34949 <i>i</i>	8.8397 - 1.2616 <i>i</i>	9.52038 - 1.34949 <i>i</i>
40	10.6204 - 1.34949 <i>i</i>	11.5075 - 1.2607 <i>i</i>	12.6938 - 1.34949 <i>i</i>
50	13.2755 - 1.34949 <i>i</i>	14.1705 - 1.2603 <i>i</i>	15.8673 - 1.34949 <i>i</i>

Table 3.8: Comparison between the eikonal approx. and the numerical values of scalar QNMs ($d = 10$, $k = 2$ and $n = 1$) (in units of 10^{-6})

Scalar		
l	ω_{eik}	ω_{num}
10	$3.51238 - 1.34949i$	$4.3254 - 1.2285i$
20	$7.02476 - 1.34949i$	$8.0203 - 1.2502i$
30	$10.5371 - 1.34949i$	$11.6034 - 1.2549i$
40	$14.0495 - 1.34949i$	$15.1536 - 1.2568i$
50	$17.5619 - 1.34949i$	$18.6895 - 1.2577i$

Table 3.9: QNMs for Tensor perturbations for various values of k with $d = 17$ and $l = 7$ (in units of 10^{-14})

n	ω ($k = 2$)	ω ($k = 3$)	ω ($k = 4$)	ω ($k = 5$)
0	7.5654 - 1.1475 <i>i</i>	7.6440 - 1.2976 <i>i</i>	9.9011 - 2.0021 <i>i</i>	15.8018 - 5.3654 <i>i</i>
1	7.0333 - 3.4599 <i>i</i>	7.2096 - 3.9518 <i>i</i>	9.3245 - 6.1374 <i>i</i>	14.0911 - 16.8858 <i>i</i>
2	5.7838 - 5.8365 <i>i</i>	6.3300 - 6.8135 <i>i</i>	8.2728 - 10.6688 <i>i</i>	12.0281 - 30.0839 <i>i</i>

Table 3.10: QNMs for Vector perturbations for various values of k with $d = 17$ and $l = 7$ (in units of 10^{-14})

n	ω ($k = 2$)	ω ($k = 3$)	ω ($k = 4$)	ω ($k = 5$)
0	7.3405 - 1.1101 <i>i</i>	8.0021 - 1.2382 <i>i</i>	12.1344 - 1.9030 <i>i</i>	31.8981 - 5.0575 <i>i</i>
1	6.8017 - 3.3424 <i>i</i>	7.5894 - 3.7559 <i>i</i>	11.6583 - 5.7797 <i>i</i>	30.8876 - 15.3589 <i>i</i>
2	5.5808 - 5.6277 <i>i</i>	6.7427 - 6.4196 <i>i</i>	10.7347 - 9.8779 <i>i</i>	29.0064 - 26.2060 <i>i</i>

Table 3.11: QNMs for Scalar perturbations for various values of k with $d = 17$ and $l = 7$ (in units of 10^{-14})

n	ω ($k = 2$)	ω ($k = 3$)	ω ($k = 4$)	ω ($k = 5$)
0	7.1050 - 1.0462 <i>i</i>	8.3319 - 1.1800 <i>i</i>	13.9275 - 1.8777 <i>i</i>	41.6200 - 5.1162 <i>i</i>
1	6.5859 - 3.1448 <i>i</i>	7.9915 - 3.5720 <i>i</i>	13.5324 - 5.6876 <i>i</i>	40.8428 - 15.4635 <i>i</i>
2	5.4291 - 5.2934 <i>i</i>	7.3036 - 6.0721 <i>i</i>	12.7618 - 9.6663 <i>i</i>	39.3575 - 26.1500 <i>i</i>

3.4 Conclusion

We have studied the quasinormal modes of metric perturbations of tensor, vector and scalar type for asymptotically flat black hole spacetimes for a particular class of theories in the Lovelock model. These theories are specified by the action given by (3.6) with the higher order coupling constants given by (3.10). We used the sixth order WKB formula for the quasinormal modes [71] in order to compute the QNMs for various values of d and k . We also used the connection between null geodesic parameters and the asymptotic quasinormal modes of static and spherically symmetric spacetimes, established in [63], to deduce an analytic form for the asymptotic modes in the limit $l \rightarrow \infty$. Numerical analysis indicates that the asymptotic behavior of the QNMs in higher ordered theories is indeed consistent with the theory, as can be seen easily from Tables 3.7 and 3.8. We observe that the imaginary parts of the modes attain a constant value for very high values of the parameter l , as suggested by the null geodesic method. We calculated the quasinormal modes of perturbations for different orders of the Lovelock theory and found that the real as well as imaginary parts of the modes increase with increasing values of k . We also found that the real parts of the modes decrease with increase in the spacetime dimension d . The theory also suggests that the modes should be approximately isospectral at high values of d . This is seen to hold roughly at $d \geq 10$, especially in the case of imaginary parts. The quasinormal behavior revealed in this chapter should help us understand better the dynamics of fields in the vicinity of black holes in higher ordered theories of gravity.

4

Thermodynamics of Charged Lovelock - AdS Black Holes

4.1 Introduction

The subject of black hole thermodynamics had its origin in the observation [74–80] of a mathematical connection between various quantities that are relevant to black hole dynamics - horizon-area, mass, surface gravity etc. and thermodynamic variables - entropy, temperature etc. that describe the thermodynamic behavior of systems. Consequences of this mathematical connection drive the current intense activity in this field, more than four decades after its initial discovery. We now suspect that this connection actually goes much deeper than a simple one-to-one correspondence between various parameters. It is known that many aspects of quantum field theories of various systems have their dual in gravitational systems. This connection enables us to analyze the behavior of such systems by studying their dual gravitational theories, which is often a much easier task. Recently discovered gauge-gravity dualities like the AdS/CFT correspondence [3], according to which asymptotically AdS gravitational theories in d dimensions are dual to quantum field theories in a $(d-1)$ dimensional sub-manifold, have fueled intense interest in asymptotically AdS spacetimes.

The occurrence of phase transitions between various black hole states is a very important aspect of thermodynamic studies of gravitational systems, since it would enable us to study the behavior of their dual systems near their critical points. These phase transitions can be studied in various ways - studying the heat capacity of black hole spacetimes is one approach [81, 88], in which the positivity of the specific heat would point to a stable phase of the black hole while a negative value signals an unstable phase. Transitions between thermal AdS space and black hole configurations, discovered by Hawking [30], is considered as the pioneering study on the subject. According to it, pure thermal radiation in AdS space becomes unstable above a certain temperature and collapses to form black holes. This is the well-known Hawking-Page phase transition which describes the phase transition between the Schwarzschild AdS black hole and the thermal AdS space. This is dual [89] to the confinement/deconfinement phase transition of gauge fields according to the AdS/CFT correspondence [3]. Since then, phase transitions of black holes have been investigated from different perspectives. Some recent works may be found in [90–110].

Another approach to analyze black hole thermodynamic stability is to apply the methods of differential geometry by considering the thermodynamic phase space of a black hole system as a Riemannian manifold and studying its curvature, which would then represent thermodynamic interaction [111–122]. This curvature is determined by assigning a metric to the thermodynamic phase space. The components of the metric are defined in terms of second derivatives of suitable thermodynamic potentials with respect to a set of extensive variables N^a of the thermodynamic system. Usual choices for the

thermodynamic potentials are the mass M , internal energy U , entropy S , etc. of the black hole spacetime. Depending on the choice of the metric, different versions of the geometric approach exist. The thermodynamic geometry method was first introduced by Weinhold [117] and Ruppeiner [118]. Weinhold proposed a metric structure in the energy representation as $g_{ij}^W = \partial_i \partial_j M(U, N^a)$, while Ruppeiner defined the metric structure as $g_{ij}^R = -\partial_i \partial_j S(U, N^a)$. Components of these metrics are those of the Hessian matrix of the internal energy M and the entropy S respectively, with respect to the extensive thermodynamic variables N^a . Weinhold's metric was found to be conformally connected to Ruppeiner's through the relation $ds_R^2 = \frac{ds_W^2}{T}$ [123], T being the horizon temperature. Ruppeiner's metric has extensively been used in the geometric analysis of various black hole spacetimes [124]. Recently, Quevedo et al. [120] presented a new formalism called geometrothermodynamics, which allows us to derive Legendre invariant metrics for the phase space. Geometrothermodynamics presents a unified geometry where the metric structure describes various types of black hole thermodynamics [119–122, 125–130].

Theoretical interest in the black hole horizon area stems from arguments [67, 131] that the origin of horizon entropy is related to the quantum structure of spacetime. Statistical mechanics tells us that entropy is a measure of the number of occupied microstates of a system that have equal probability of being occupied. The direct counting of these microstates in the case of black hole spacetimes is still an unresolved problem. On one hand, entropy must obey the second law of thermodynamics, according to which it can do nothing but increase. On the other hand, we also know from the no - hair theorem that the state of the black hole systems must be specified

by a mere handful of parameters, namely the mass M , the charge Q and the angular momentum J of the black hole. In other words, a large portion of information regarding the fields that collapse to form black holes get lost to the observable universe, so that the nature of the microstates becomes obscure. This leads to a violation of unitarity since, according to quantum mechanics, pure states can only evolve into pure states, whereas the state inside the black hole becomes mixed after its formation. There have been suggestions [133] that gravitational collapse could lead to the formation of topologically disconnected regions where the information could be stored. Thus, black hole horizon area is considered to be intimately related to the very process of black hole formation and could offer vital glimpses into the quantum nature of spacetime itself, and thus be of incredible help in the formulation of a quantum theory of gravity. Following the initial proposal of Bekenstein [38, 135, 136] of the discrete nature of the black hole spectrum, various approaches have been developed for the computation of the same [42, 43, 52, 137–144].

In the present chapter, we test the thermodynamic stability of black holes in charged, asymptotically AdS, spherically symmetric spacetimes in Lovelock model. Ordinary thermodynamic analysis reveals the existence of two points in charged spacetimes, where the specific heat as a function of the horizon radius diverges, compared to just one in the uncharged case. Then we compute the scalar curvature of the thermodynamic phase space for the spacetime using a Legendre-invariant metric proposed by Quevedo [119] and find that there exist divergences in the scalar curvature near the points of divergence of the specific heat, thus explaining the thermodynamic phase transitions. We then calculate the area spectrum of black hole horizons in the

model by directly calculating the adiabatic invariant for the spacetime and applying the Bohr-Sommerfeld quantization condition to it. A brief outline of the paper is as follows: in Sect. 4.2, we explain the maximally symmetric Lovelock model and the resulting metric for the charged AdS black hole spacetime [50]. We also calculate the relevant thermodynamic quantities like the horizon temperature, entropy and the specific heat in the same section. Details of the geometrothermodynamic method of analyzing the phase transitions are given in Sect. 4.3. Calculation of the adiabatic invariant for the spacetime and the deduction of the area spectrum of large black hole are performed in Sect. 4.4. The results are summarized in Sect. 4.5.

4.2 Thermodynamic Stability of Charged AdS Black Holes in Lovelock Model

The Lovelock model of gravity [14, 145] is developed based on a Lagrangian in the form of a polynomial in the Riemann curvature. The degree of the polynomial determines the order of the resulting theory. It is known [10, 13, 19] that the stability of the solutions to these theories against metric perturbations is not always guaranteed. The black hole spacetimes, whose thermodynamic stability is studied in the present work, are solutions to a subset of the general Lovelock theories, restricted by the additional constraint that all the solutions must possess a unique AdS vacuum state with a fixed cosmological constant [50]. In such theories, the order k of the corresponding Lagrangian labels the different theories and it is seen that the type of the theory depends on the values of k and dimension d of the spacetime. For $d > 3$, the metric representing the spherically symmetric, charged, asymptotically AdS solutions to such theories, is given by

[50],

$$ds^2 = -f(r)dt^2 + \frac{dr^2}{f(r)} + r^2 d\Omega_{d-2}^2, \quad (4.1)$$

where $f(r)$ is given by

$$f(r) = 1 + \frac{r^2}{R^2} - g(r), \quad \text{where} \quad (4.2)$$

$$g(r) = \left[\frac{2G_k M}{r^{d-2k-1}} - \left(\frac{\epsilon G_k}{d-3} \right) \frac{Q^2}{r^{2(d-k-2)}} \right] \frac{1}{k}.$$

Here, r is a Schwarzschild - like coordinate and R is the unique AdS radius, related to the cosmological constant Λ by the relation $\Lambda = -\frac{(d-1)(d-2)}{2R^2}$. The constant ϵ is proportional to the permeability of the vacuum. The value of R is taken to be equal to 1 for all the numerical calculations in this paper. G_k refers to the gravitational constant for the theory of order k . The constants M and Q refer to the mass and the electric charge of the black hole respectively. It is also known [50] that there exists a lower limit for the mass of the black hole M and the size r_e of the charged object, as long as we wish to avoid time - like singularities.

The event horizon r_+ of the black hole is taken as the largest positive root of the equation $f(r) = 0$. For arbitrary values of the parameters d and k , it is obviously not possible to express r_+ as a function of the parameters M , Q , R , etc. However, it is possible to express the mass M of the black hole as a function of r_+ , which is plotted in Fig. 4.1. The function M is expressed in terms of r_+ as,

$$M(r_+) = \frac{r_+^{d-2k-1}}{2G_k} \left[\left(1 + \frac{r_+^2}{R^2} \right)^k + \left(\frac{\epsilon G_k}{d-3} \right) \frac{Q^2}{r_+^{2(d-k-2)}} \right]. \quad (4.3)$$

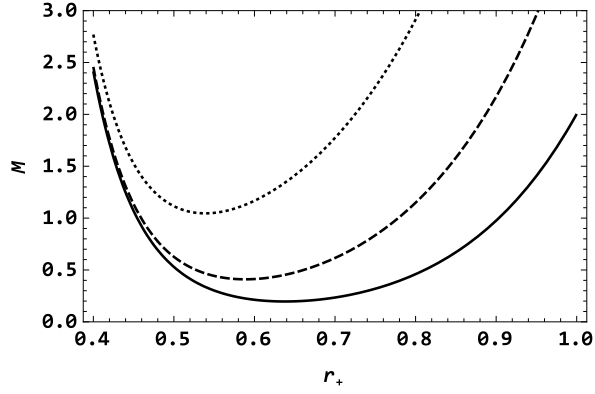


Figure 4.1: Mass of the charged black hole as a function of r_+ . The curves are drawn for $d = 10$ and $Q = 0.235$, with $k = 2$ (solid), $k = 3$ (dashed) and $k = 4$ (dotted).

The horizon temperature T is obtained by requiring the Euclidean time to be periodic with period $\tau = 4\pi \left(\frac{df}{dr} \Big|_{r=r_+} \right)^{-1}$ and equating it to $\frac{1}{\kappa_B T}$, κ_B being the Boltzmann constant. We can easily see that, for the charged black holes, the horizon temperature is given by

$$T(r_+) = \frac{1}{4\pi\kappa_B} \frac{df}{dr} \Big|_{r=r_+} = \frac{2r_+}{R^2} - \frac{1}{k} \left[g(r_+) \right]^{\frac{1}{k}-1} \times g'(r_+). \quad (4.4)$$

Eq.(4.4) represents a non-monotonic function having a couple of turning points when expressed as a function of r_+ . Once again, it

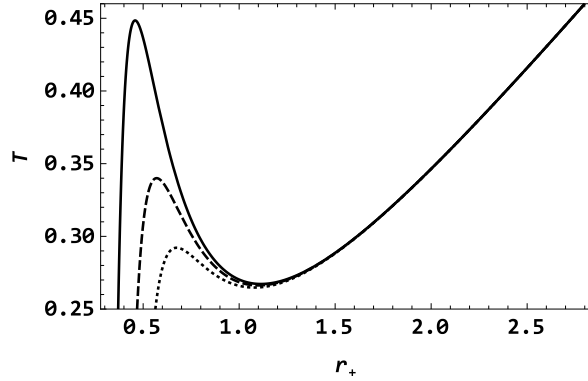


Figure 4.2: Temperature of the charged black hole as a function of r_+ , for $d = 7$, $k = 2$. The curves are drawn for $Q = 0.2$ (solid), $Q = 0.3$ (dashed) and $Q = 0.4$ (dotted).

is not possible to obtain closed-form expressions for these points in terms of the black hole parameters, as long as the dimension d and order k are not fixed. However, one can analyze the behavior of $T(r_+)$ as a function of r_+ graphically. Fig. 4.2 represents a plot between $T(r_+)$ and r_+ . From the plot, it is obvious that one of the turning points represents a maximum while the other is a minimum. The existence of a minimum of $T(r_+)$ is known already in the case of uncharged black holes [50], while the existence of the maximum appears to be unique to the charged case.

The function $S(r_+)$, representing the entropy of the black hole event horizon as a function of the horizon radius r_+ is obtained in the general case of a Lovelock theory of order k at spacetime dimension d by evaluating the Euclidean action for the black hole spacetime and equating it to β times the free energy of the system, where β is defined by the expression $\left. \frac{df}{dr} \right|_{r_+} = 4\pi\beta^{-1}$. After some calculation, it is seen

that the entropy $S(r_+)$ is given by,

$$S(r_+) = \frac{r_+^{d-2k}}{d-2k} {}_2F_1\left(\frac{1}{2}(d-2k), 1-k; \frac{1}{2}(d-2k+2); -\frac{r_+^2}{R^2}\right), \quad (4.5)$$

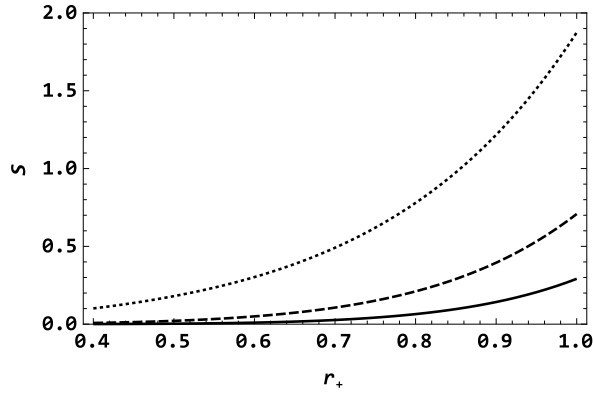


Figure 4.3: Entropy of the charged black hole as a function of r_+ . The curves are drawn for $d = 10$ and $Q = 0.235$, with $k = 2$ (solid), $k = 3$ (dashed) and $k = 4$ (dotted).

where ${}_2F_1$ represents the hypergeometric function. Graphically, it is seen from Fig. 4.3 that $S(r_+)$ is a monotonically increasing function of r_+ . For $k = 1$, it can readily be seen that $S(r_+) \propto r_+^{d-2}$, which is nothing but the usual area law, namely $S \propto A$, A being the horizon-area. Also, $S(r_+)$ becomes proportional to the area for $k \neq 1$ theories when $r_+ \gg R$, i.e. for very large black holes.

In order to investigate the thermodynamic stability of the black hole spacetime, we compute the specific heat C_p for the spacetime, defined as $C_p = \frac{\partial M}{\partial T}$. Since both M and T can conveniently be expressed as functions of r_+ , we compute C_p also as a function of r_+

using the expression $C_p(r_+) = \frac{\partial_{r_+} M}{\partial_{r_+} T}$. The explicit form of the function turns out to be too long to include here, so that we resort to graphical analysis.

In all dimensions d and for all orders k , we find that there exists a range of values for the parameter Q , for which the function $T(r_+)$ has a couple of turning points. Since $C_p(r_+) = \frac{\partial_{r_+} M}{\partial_{r_+} T}$, we expect to find two points of divergence when we plot C_p against r_+ , indicating points at which C_p changes sign discontinuously, signaling transitions between stable (+ve value for C_p) and unstable (-ve values for C_p) phases. This indeed turns out to be the case. We name the two turning points of $T(r_+)$ as r_{c1} (the maximum) and r_{c2} (the minimum). Samples of the typical variation of C_p with r_+ in the vicinity of r_{c1} and r_{c2} , for one particular set of values for the parameters d and Q with different values for k , are plotted in Figs. 4.4 and 4.5 respectively. From the analysis of the plots of C_p against r_+ for various combinations of d , k and Q , we observe that, when r_+ decreases, the transition at r_{c2} is always from a stable phase to an unstable phase, whereas the nature of the transition at r_{c1} changes from case to case, depending on the values of d , k and Q . For example, it is clear from Fig. 4.4 that the second order theory (solid curve) in a ten dimensional spacetime predicts a stable-to-unstable transition, while the third order theory (dashed curve) predicts a unstable-to-stable transition at r_{c1} when r_+ decreases. In those cases where the transition at r_{c1} is from a stable phase to an unstable phase, such as the one depicted by the solid curve in Fig. 4.4, there obviously occurs a continuous sign-change in $C_p(r_+)$, as clearly seen in the figure.

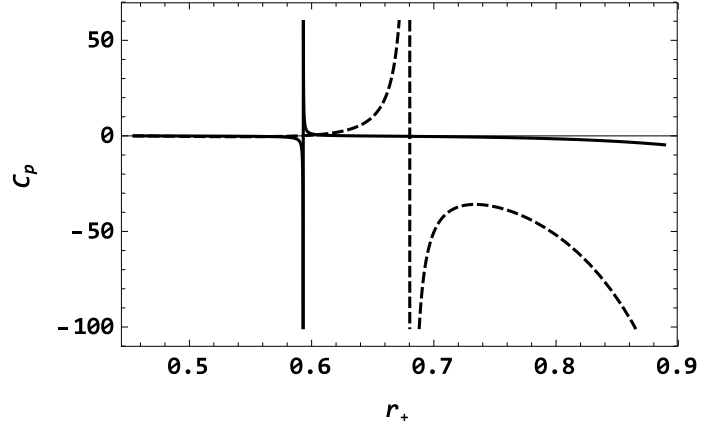


Figure 4.4: $C_p - r_+$ variation in the vicinity of r_{c1} . The curves are drawn with $d = 10$, $k = 2$ (solid) and $d = 10$, $k = 3$ (dashed). In both cases, $Q = 0.235$

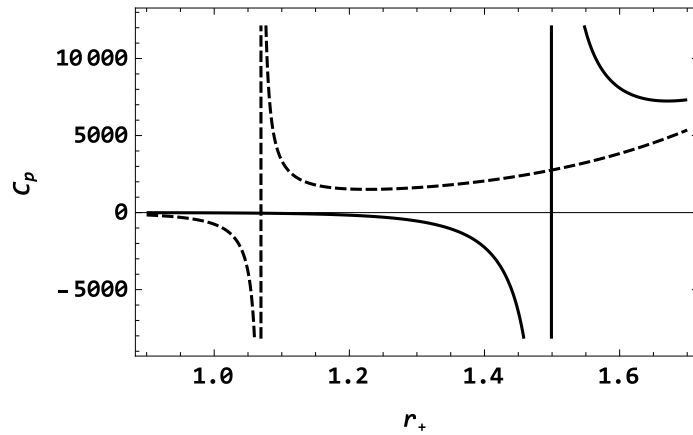


Figure 4.5: $C_p - r_+$ variation in the vicinity of r_{c2} . The curves are drawn with $d = 10$, $k = 2$ (solid) and $d = 10$, $k = 3$ (dashed). In both cases, $Q = 0.235$

We now take another case and analyze the thermodynamic behavior in some more detail. We select a black hole spacetime with $d = 7$, $k =$

2 and $Q = 0.235$. Plots of C_p against r_+ in the neighborhood of r_{c1} and r_{c2} are given in Fig. 4.6 and 4.7. From the figures, it is obvious that, for this particular case, as r_+ decreases, the transition at r_{c2} is from a stable phase to an unstable phase, whereas the transition at r_{c1} is from an unstable phase to a stable one.

Let us try to analyze the thermodynamic stability of the spacetime using Figs. 4.6-4.8. We will see that the thermodynamic stability depends on both the size of the black hole and the temperature of the background AdS spacetime. The thermodynamic behavior of the black holes depends crucially on whether the temperature (T_0) of the background spacetime (also called thermal bath) is **(i)** larger than the local maximum value (T_{max}) of $T(r_+)$, **(ii)** between T_{max} and the local minimum value (T_{min}) of $T(r_+)$, or **(iii)** lower than T_{min} . Another important factor that determines the thermodynamic behavior in all these three cases is the size r_+ of the black hole itself - whether it is greater than r_{c2} , in between r_{c2} and r_{c1} or less than r_{c1} . We analyze some of the possible scenarios here:

Case (i) - $T_0 > T_{max}$:

In this case, we see that, similar to the case of Schwarzschild-AdS black holes, very large black holes in the model can always attain equilibrium with an external thermal bath at a finite temperature, since the specific heat is positive in this region. There is one difference though - when r_+ is large and the temperature T_0 of the bath is higher than the maximum value of $T(r_+)$, a straight line parallel to the horizontal axis meets the $T(r_+) - r_+$ curve at only one point, which means that there exists only one final, stable, equilibrium

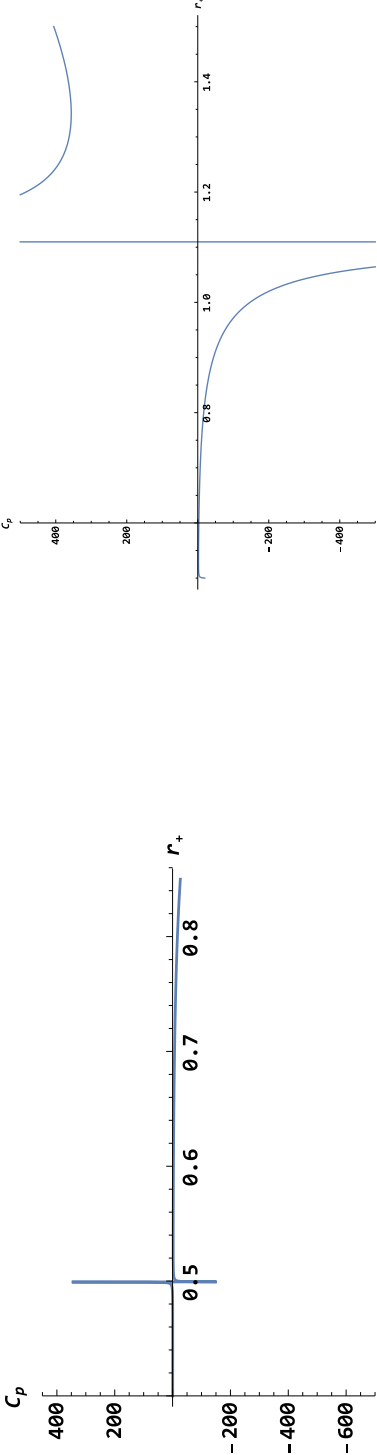


Figure 4.6: Divergence of $C_p(r_+)$ at r_{cl1} , with $d = 7$, $k = 2$ and $Q = 0.235$

Figure 4.7: Divergence of $C_p(r_+)$ at r_{cl2} , with $d = 7$, $k = 2$ and $Q = 0.235$

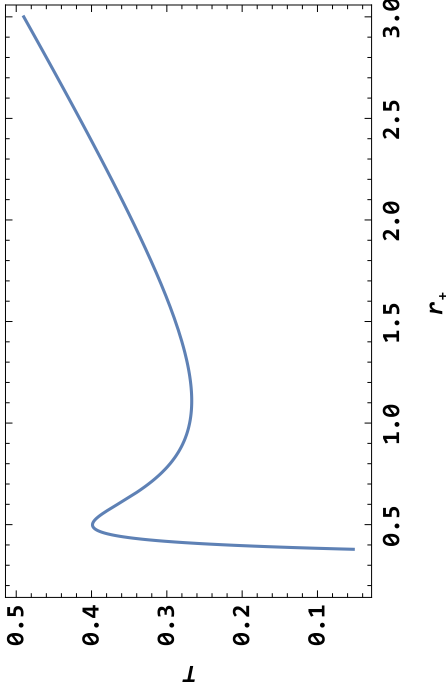


Figure 4.8: Variation of T with r_+ for $d = 7$, $k = 2$ and $Q = 0.235$

configuration for such a black hole at that background temperature, with a horizon radius which is larger than r_{c2} . This is not the case for uncharged black holes - the uncharged spacetime always has two equilibrium configurations - one being unstable and the other being stable - as long as the temperature of the bath is higher than the minimum of $T(r_+)$ [50]. Thus, for the charged case, a black hole with $r_+ > r_{c2}$ will get drawn towards the equilibrium state at temperature T_0 , since the specific heat is positive for $r_+ > r_{c2}$.

Case (ii) - $T_0 < T_{min}$:

Charged AdS Lovelock black holes can attain equilibrium with a thermal bath of *any* positive temperature, whereas the uncharged ones are known [50] to be unable to attain equilibrium with a bath of temperature lower than the minimum of $T(r_+)$. Case (ii) is an example of such a scenario. Here again, there exists only one thermodynamically stable equilibrium configuration that the small black holes can get drawn towards, since the straight line parallel to the horizontal axis still cuts the $T(r_+) - r_+$ curve at only one point. In this case, the horizon radius for the equilibrium state will be smaller than r_{c1} . The specific heat is positive in the region $r_+ < r_{c1}$, so that a black hole with $r_+ < r_{c1}$ tends to make a transition towards this equilibrium state rather than away from it.

Case (iii) - $T_{min} < T_0 < T_{max}$:

It is clear from Fig. 4.8 that, in this range, each value of T_0 corresponds to three equilibrium states of different radii - say, r_{s1} (less than r_{c1} , corresponding to a locally stable state), r_u (in between r_{c1} and r_{c2} ,

corresponding to an unstable state) and r_{s2} (larger than r_{c2} , corresponding to a locally stable state). The points r_{s1} and r_{s2} exist in regions with positive specific heat, as clearly seen from Figs. 4.6 and 4.7 so that initial black hole states with $r_+ < r_{c1}$ and $r_+ > r_{c2}$ are drawn towards these equilibrium points respectively. On the other hand, the point r_u exists in a region with negative specific heat, so that initial black hole states with $r_{c1} < r_+ < r_{c2}$ are drawn away from this equilibrium point. Thus, if the temperature of the thermal bath falls in the range $T_{min} < T_0 < T_{max}$, the resultant thermodynamic behavior of the black hole will depend on its initial size. Essentially, initial black hole states with $r_+ > r_u$ will evolve towards an equilibrium configuration with $r_+ = r_{s2}$ and those with $r_+ < r_u$ will tend to evolve towards a configuration with $r_+ = r_{s1}$. This is in contrast with the uncharged case, where a black hole with an initial size $r_+ < r_u$ can never reach equilibrium [50].

The occurrence of a phase transition in this sample case is also indicated by a plot between the Gibbs free energy $F(r_+) = M(r_+) - T(r_+)S(r_+)$ and the horizon temperature T , given in Fig. 4.9. The presence of a cusp in the plot indicates that there occurs a second order phase transition in the black hole spacetime.

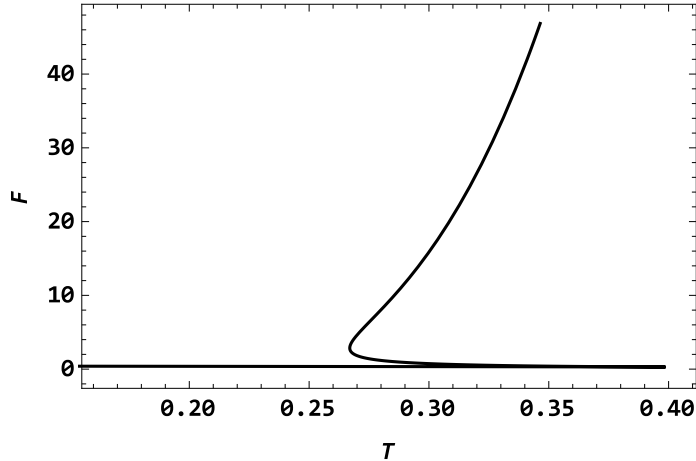


Figure 4.9: Free energy of the charged black hole as a function of r_+ for $d = 7$, $k = 2$ and $Q = 0.235$

4.3 Geometrothermodynamic (GTD) Analysis

We employ the Legendre invariant method of Quevedo [119–122, 146, 147] in order to study the phase transition in the geometric formalism. We choose the entropy representation, in which the Ricci scalar R_R that represents the thermodynamic interaction of the system is derived from a thermodynamic metric which is defined in terms of the second derivatives of the entropy S of the system, considered as a function of the relevant extensive parameters. For our spacetime representing the charged, AdS Lovelock black holes, we take M and Q as the extensive parameters. Since M can conveniently be expressed as a function of the horizon radius r_+ , we take $M = M(r_+)$, $Q = Q(r_+)$, $S = S(r_+)$ and compute the Ricci scalar R_R as a function of r_+ . Identifying M, Q as the set of extensive thermodynamic vari-

ables and $S(M, Q)$ as the thermodynamic potential Φ of the system, the Legendre invariant thermodynamic metric g^Q is computed using the relation,

$$g^Q = \begin{pmatrix} g_{11} & 0 \\ 0 & g_{22} \end{pmatrix}, \quad (4.6)$$

where g_{11} and g_{22} are given by,

$$g_{11} = - \left(M \frac{\partial_r S}{\partial_r M} + Q \frac{\partial_r S}{\partial_r Q} \right) \left(\frac{\partial_r M \partial_{rr} S - \partial_r S \partial_{rr} M}{(\partial_r M)^3} \right), \text{ and} \quad (4.7)$$

$$g_{22} = \left(M \frac{\partial_r S}{\partial_r M} + Q \frac{\partial_r S}{\partial_r Q} \right) \left(\frac{\partial_r Q \partial_{rr} S - \partial_r S \partial_{rr} Q}{(\partial_r Q)^3} \right). \quad (4.8)$$

Note that the symbol r replaces r_+ in (4.7) and (4.8). Although the analytic calculation is straightforward, the resultant expressions for the metric-components and that of the Ricci scalar R_R are too long to be explicitly included here. Therefore, we resort to numerical analysis and study the behavior of R_R graphically as a function of r_+ . In Figs. 4.10-4.13, we plot $R_R(M, Q)$ against r_+ for specific values of the black hole parameters and compare it with the corresponding plots of the heat capacity C_p , also plotted against r_+ in exactly the same range. From the plots, it is clear that the divergences in R_R occur at points which are very near to those at which the heat capacity diverges. Hence, we conclude that the usual thermodynamic approach and the GTD method are in agreement in predicting the thermodynamic behavior of the black hole spacetime.

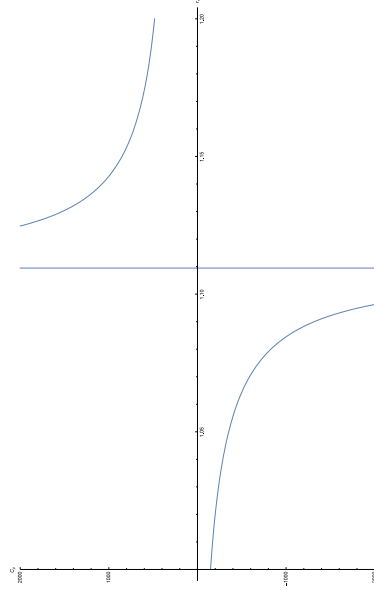


Figure 4.11: Divergence of $C_p(r_+)$ at r_{c2} . Here, $d = 7$, $k = 2$ and $Q = 0.235$

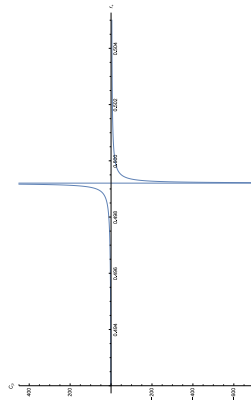


Figure 4.10: Divergence of $C_p(r_+)$ at r_{c1} . Here, $d = 7$, $k = 2$ and $Q = 0.235$

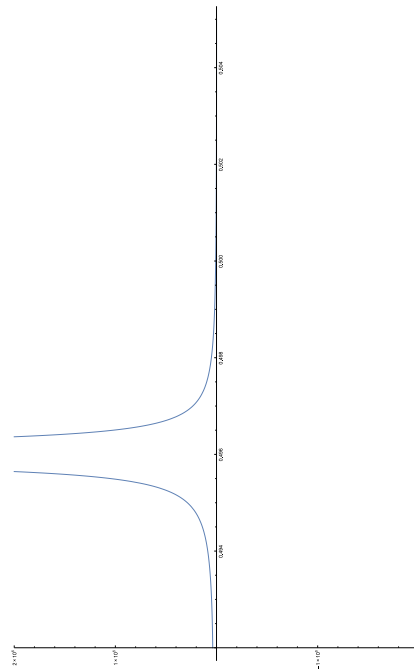


Figure 4.12: Divergence of R_R near r_{cl} .
Here, $d = 7$, $k = 2$ and $Q = 0.235$

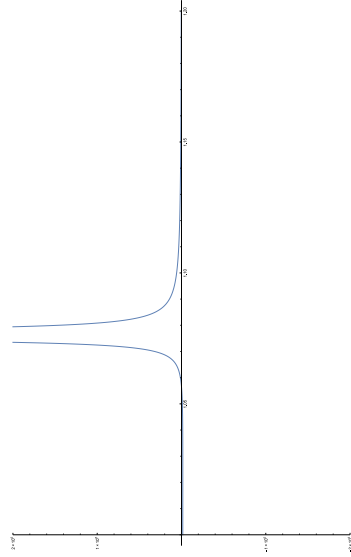


Figure 4.13: Divergence of R_R near r_{c2} .
Here, $d = 7$, $k = 2$ and $Q = 0.235$

4.4 Area Spectrum of Large Charged AdS Black Holes in Lovelock Model

In this section, we compute the horizon area spectrum of large ($r_+ \gg R$) charged, AdS black holes in Lovelock model. The fact that horizon area of black holes is quantized was proposed for the first time by Bekenstein [38, 135, 136]. He found that the horizon area of a non-extremal black hole is a classical adiabatic invariant. It is known from field theory (Ehrenfest Principle) that the presence of a periodicity in the classical theory of a system points to the existence of an adiabatic invariant with a discrete spectrum in the corresponding quantum theory. We follow the recent proposal by Majhi and Vagenas [148] that the quantity $I = \sum \int p_i dq_i$ can be taken as the classical adiabatic quantity in the case of black hole spacetimes, where q_i and p_i are conjugate variables describing the dynamics of the system.

For a spacetime whose metric is given by

$$ds^2 = f(r)d\tau^2 + \frac{1}{f(r)}dr^2 + r^2 d\Omega_{d-2}^2, \quad (4.9)$$

where $\tau = it$ is the Euclidean time coordinate, we take $q_0 = \tau$ and $q_1 = r_h$ as the dynamical variables of the system and consider the Hamiltonian H as a function of q_i and p_i . Then, taking into account one of the Hamiltonian equations of motion of the system, namely, $p_i = \frac{\partial H}{\partial \dot{q}_i}$, it is possible to show that the adiabatic invariant I for the spacetime takes the form,

$$I = -2i \int \int_0^H \frac{dH'}{f(r)} dr. \quad (4.10)$$

Near the horizon r_h , we can approximate $f(r) \approx \kappa(r - r_h)$, where $\kappa = \left. \frac{df}{dr} \right|_{r=r_h}$. Also, the temperature T of the horizon is given by $T = \frac{1}{4\pi} \kappa$. Substituting all these into (4.10), we get,

$$I = \frac{1}{2} \int_0^H \frac{dH'}{T}. \quad (4.11)$$

Considering the black hole spacetime as a thermodynamic system with extensive variables S and Q , we equate the Hamiltonian H' to the mass M of the black hole, so that the first law of thermodynamics reads

$$dH' = dM = TdS + \Phi dQ, \quad (4.12)$$

$\Phi = \frac{\partial M}{\partial Q}$ being the electric potential. Thus, (4.11) gives

$$I = \frac{1}{2} (S + \int_0^Q \frac{\Phi}{T} dQ'). \quad (4.13)$$

The temperature T of the horizon is given by $T = \frac{1}{4\pi} \left. \frac{df}{dr} \right|_{r=r_h}$, and $\Phi = \frac{\partial M}{\partial Q'}$, where $M(Q')$ by replacing Q with Q' in (4.3). We get

$$\Phi = \frac{\epsilon r_h^{3-d}}{d-3} Q'. \quad (4.14)$$

We compute the second term on the RHS of (4.13) after substituting the values of Φ and T . Its value turns out to be,

$$\int_0^Q \frac{\Phi}{T} dQ' = \frac{a}{2c} \ln(b - c Q^2), \text{ where} \quad (4.15)$$

$$a = \frac{\epsilon r_h^{3-d}}{d-3},$$

$$b = \frac{1}{4\pi} \left[\frac{2r_h}{R^2} + \frac{2G_k M(d-2k-1)}{kr_h^{d-2k}} \left(1 + \frac{r_h^2}{R^2} \right)^{1-k} \right], \text{ and}$$

$$c = \frac{1}{4\pi} \left[\frac{2\epsilon G_k(d-k-2)}{k(d-3)r_h^{2(d-k)-3}} \left(1 + \frac{r_h^2}{R^2} \right)^{1-k} \right].$$

Thus, (4.13) gives,

$$S = 2I - \frac{a}{2c} \ln(b - c Q^2)$$

According to Bohr-Sommerfeld quantization condition, $I = n\hbar$, so that we can write

$$S = 2n\hbar - \frac{a}{2c} \ln(b - c Q^2). \quad (4.16)$$

Now, it is to be noted that the usual area law, namely $S \propto A$, is unique to first order theories of gravity like the General Theory of Relativity, for which the order parameter $k = 1$. In general, the area law is not followed by black hole spacetimes in theories where $k \neq 1$. However, the area law can approximately be recovered in these theories if we restrict our attention to very large black holes, i.e. those with $r_+ \gg R$. For such black holes, the general expression for the entropy for $S(r_+)$, given by (4.5), reduces to

$$S(r_+) \approx k \left(\frac{2\pi\kappa_B}{(d-2)G_k R^{2(k-1)}} \right) r_+^{d-2}, \quad (4.17)$$

which can be written in terms of the area A of the event horizon as

$$S(r_+) \approx k \left(\frac{2\pi\kappa_B}{(d-2)G_k R^{2(k-1)}} \right) \left(\frac{A}{\Omega_{d-2}} \right). \quad (4.18)$$

Using (4.18) in (4.16), we can write an expression for the quantized area of large, charged black holes in the asymptotically AdS Lovelock model as,

$$A = \gamma \left(n\hbar - \frac{a}{4c} \ln (b - c Q^2) \right), \quad (4.19)$$

where the constant γ is given by,

$$\gamma = \frac{(d-2)\Omega_{d-2}G_k R^{2(k-1)}}{\pi\kappa_B}.$$

Thus the horizon-area of large, charged, black holes in the model turns out to be quantized, with a logarithmic correction term added to it. The dependence of the area-quantum on the order of the theory k and the AdS radius R is evident from the expression for γ . It is to be noted that the dependence on R becomes evident only when one considers theories with $k \neq 1$. It is interesting to note that the logarithmic correction term itself does not turn out to be quantized.

4.5 Conclusions

In this chapter, we considered the thermodynamic behavior of charged, asymptotically AdS and spherically symmetric black hole solutions of the Lovelock model of gravity, where the higher-order coupling constants are chosen so as to make the AdS radius R equal for all orders. The main objective has been to investigate the thermodynamic stability of such black holes and to look for possible phase transitions between various black hole states. Two approaches were adopted toward that end - (1): the usual thermodynamic approach in which one computes the specific heat of the spacetime and looks for divergences which signal the occurrence of second order phase transitions between various states, and (2): the method of geometrothermodynamics, in

which one studies the thermodynamic interaction of the black hole by applying methods of differential geometry to the thermodynamic phase space of the system.

Using the usual methods of black hole thermodynamics, we calculated different thermodynamic parameters of the system such as the horizon temperature, entropy and the specific heat. We found that the horizon temperature T , when written as a function of the horizon radius r_+ , has a couple of turning points, compared to just one in the uncharged case. Entropy S happens to be a monotonic function of r_+ , while the specific heat C_p exhibits divergence at two points corresponding to the turning points of $T(r_+)$. From the plots of $T(r_+)$ and $C_p(r_+)$ against r_+ , we were able to deduce the thermodynamic behavior of the black holes.

We found that large black holes are always able to attain thermodynamic equilibrium with the background AdS spacetime (the thermal bath) as long as the bath has a temperature greater than the local maximum value of $T(r_+)$. In this case, there exists only one stable equilibrium configuration for a black hole at any bath temperature T_0 . A similar conclusion can be arrived at in the case of small black holes placed inside a bath at a temperature T_0 that is less than the local minimum value of $T(r_+)$. There exists a stable equilibrium configuration in this case as well, in contrast with the case of uncharged black holes. In this case, as in the previous case, initial black hole states get drawn towards the respective equilibrium configurations, since the specific heat is positive in both cases. When the temperature of the bath is in between the local maximum and local minimum values of $T(r_+)$, each bath temperature T_0 corresponds to three equi-

librium black hole configurations - two stable states and one unstable state. In such a case, we concluded that initial black hole configurations would be drawn towards one of the stable points, depending on their initial size.

In order to perform the geometric analysis of the thermodynamic evolution, we followed the method of geometrothermodynamics of Quevedo [119, 120]. We chose what is known as the entropy representation of the thermodynamic phase space and computed the scalar curvature R_R derived from a Legendre invariant thermodynamic metric, the components of which are calculated using the second derivatives of the entropy of the system. We chose the mass and the charge of the black hole as the extensive parameters. Since the expressions for the metric components and the scalar curvature were too long to treat analytically, we resorted to the graphical method, plotting the scalar curvature as a function of the horizon radius r_+ . From the plot, we found that the scalar curvature diverges at points that are very close to the points of divergence of the specific heat of the black hole, indicating that the thermodynamic phase transitions of the black hole correspond to the singularities in the corresponding thermodynamic phase space. Thus, the results of geometrothermodynamics were found to be in agreement with those of ordinary black hole thermodynamics.

Next, we computed the horizon area spectrum of large, charged AdS black holes in the model, motivated mainly by the AdS/CFT correspondence. We computed the adiabatic invariant $\sum \int p_i dq_i$ for the black hole spacetime taking the Euclidean time $\tau = it$ and the horizon radius r_h as the dynamical variables. The first law of thermo-

dynamics was made use of during the computation. We applied the Bohr-Sommerfeld quantization rule to the invariant and found that the entropy is a quantized entity with a logarithmic correction term added to it. In the limit of large black holes, the entropy becomes proportional to the horizon area for higher order Lovelock theories and we were able to show that the area of such black holes also can be written as a quantized number with a logarithmic correction term added to it. The spacing γ between the various quanta was found to be dependent on the order k of the theory (and by extension the dimension d of the spacetime) and the value of the AdS radius R , although this dependence become evident only in higher dimensions and higher order theories.

5

Summary

The idea that we may be living in a higher - than - four dimensional universe is something that could very well be justified based on a purely intellectual, egalitarian point of view - one could argue that the number 4 must not be given any special status as the default choice for the number of spacetime dimensions and that the final word on the dimensionality of the spacetime of our universe must be based on agreement between theory and experiment. There are, however, practical reasons as well for taking higher dimensional gravity seriously, the benefits obtained from gauge - gravity duality being only one of them. The pursuit for a fully consistent, quantized theory of gravity is still an ongoing one and the most promising choices can only be consistent in higher dimensional spacetime. Add to this the prediction of the creation of micro black holes in high energy particle colliders like the LHC, and we have more than enough motivation to study physics in the background of higher dimensional black holes. Of course, when we consider gravity in higher dimensions, the General Theory of Relativity stops being the most general theory and one has to look for more general models. The most obvious choice would be to consider theories obtained from Lagrangians of higher - than - one order, among which the Lovelock model deserves special attention for reasons mentioned elsewhere in the thesis.

This thesis is a record of numerical as well as analytical investigations into the dynamics of physical fields in the vicinity of higher dimensional black holes and their thermodynamic behavior. The dynamic behavior is studied by computing the quasinormal frequencies of perturbations and the thermodynamic properties is studied by studying the stability of the event horizons against phase transitions. Methods of differential geometry were also utilized in order to verify the conclusions deduced from methods of ordinary black hole thermodynamics.

The main conclusions, in the order that they appear in the thesis, are briefly summarized below. Detailed discussions can be found in the concluding sections of the corresponding chapters.

In Chapter 2, we studied the modes of evolution of massless scalar fields in the asymptotically AdS spacetime surrounding maximally symmetric black holes of large and intermediate size in the Lovelock model. It was observed that all modes are purely damped at higher orders. Also, the rate of damping was seen to be independent of order at higher dimensions. The asymptotic form of these frequencies for the case of large black holes was found analytically. Finally, the area spectrum for such black holes was deduced from these asymptotic modes and it was found that the area quantum is actually dependent on not only the dimension d of the spacetime, but also on the order k of the theory, a feature observed only in higher order theories.

In Chapter 3, the quasinormal modes of metric perturbations in asymptotically flat black hole spacetimes in the Lovelock model were calculated for different spacetime dimensions and higher orders of

curvature. It was analytically established that in the asymptotic limit $l \rightarrow \infty$, the imaginary parts of the quasi normal frequencies become constant for tensor, scalar as well as vector perturbations. Numerical calculation showed that this indeed is the case. Also, the real and imaginary parts of the quasinormal modes were seen to increase as the order of the theory k increases. The real parts of the modes were seen to decrease as the spacetime dimension d increases, indicating the presence of lower frequency modes in higher dimensions. Also, it was seen that the modes are roughly isospectral at very high values of the spacetime dimension d .

In Chapter 4, we investigated the thermodynamic behavior of maximally symmetric charged, asymptotically AdS black hole solutions of Lovelock gravity. We explored the thermodynamic stability of such solutions by the ordinary method of calculating the specific heat of the black holes and investigating its divergences which signal second order phase transitions between black hole states. We then utilized the methods of thermodynamic geometry of black hole spacetimes in order to explain the origin of these points of divergence. We calculated the curvature scalar corresponding to a Legendre - invariant thermodynamic metric of these spacetimes and found that the divergences in the black hole specific heat correspond to singularities in the thermodynamic phase space. We also calculated the area spectrum for large black holes in the model by applying the Bohr - Sommerfeld quantization to the adiabatic invariant calculated for the spacetime.

5.1 Prospects of Future Work

In this thesis, we have investigated the dynamics of physical fields in the vicinity of black holes in higher dimensional spacetimes and the thermodynamic behavior of the black hole event horizons in higher dimensions. The background spacetimes in all these studies have been static, maximally symmetric solutions of the Lovelock model of gravity. In other words, we have only considered non - rotating black holes in this thesis. Therefore, one obvious method of extending the works in other directions would be to consider stationary solutions - rotating black holes and to study the effects of the rotation of the black hole on the physics of fields in their vicinity as well as on their horizon thermodynamics.

The AdS/CFT correspondence also provides an avenue for extending the works. According to the correspondence, there exist parallels between gravitational systems and condensed matter physics [65], which could be exploited in order to gain insight into phenomena like high - temperature superconductivity. Investigating the behavior of holographic superconductors in the background spacetimes considered in this thesis would certainly be worthwhile because of the insight it would provide into how dimension of the spacetime affects relevant parameters like the critical temperature.

The study of gravitational waves in the Lovelock models studied in this thesis is yet another direction in which the works could be extended. One would certainly like to know if the gravitational waves emitted by phenomena like black hole merger carry any “signature” regarding the spacetime dimension. The spacetimes considered in this

thesis could act as candidate models for higher dimensional spacetimes in such studies.

References

- [1] S. Dimopoulos and G. Landsberg, *Phys. Rev. Lett.* **87**, 161602 (2001)
- [2] S.B Giddings and S. Thomas, *Phys. Rev. D* **65**, 056010 (2002)
- [3] J. Maldacena, *Adv. Theor. Math. Phys.* **2**, 231 (1998)
- [4] R. Emparan and H. S. Reall, *Phys. Rev. Lett.* **88**, 101101 (2002)
- [5] G.W. Gibbons et al., *Phys. Rev. Lett.* **89**, 041101 (2002)
- [6] C. Bohm, *Invent. Math.* **134**, 145 (1998)
- [7] R. L. Bishop, *Notices Amer. Math. Soc.* **10**, 363 (1963)
- [8] G. Gibbons and S.A. Hartnoll, *Phys. Rev. D* **66**, 064024 (2002)
- [9] S.A. Hartnoll, *JHEP* **08**, 019 2003
- [10] T. Takahashi and J. Soda, *Phys.Rev.D* **79**, 104025 (2009)
- [11] A. Ishibashi and H. Kodama, *Prog. Theor. Phys.* **110**, 901–919 (2003)
- [12] H. Kodama et al., *Phys. Rev. D* **62**, 064022 (2000)
- [13] T. Takahashi and J. Soda, *Phys. Rev. D* **80**, 104021 (2009)
- [14] J.T. Wheeler, *Nuclear Physics B* **273**, 732 - 748 (1986)
- [15] D. Lovelock, *J. Math. Phys. (N.Y.)* **12**, 498 (1971)
- [16] T. Takahashi and J. Soda, *Prog. Theor. Phys.* **124**:911-924 (2010)
- [17] A. Ishibashi and R. M. Wald, *Class. Quantum Grav.* **20**, 3815 - 3826 (2003)

-
- [18] A. Ishibashi and R. M. Wald, *Class. Quantum Grav.* **21**, 2981 - 3013 (2004)
- [19] T. Takahashi and J. Soda, *Prog.Theor.Phys.* **124**:711-729 (2010)
- [20] G. Dotti, J. Oliva and R. Troncoso, *Phys. Rev. D* **75**, 024002 (2007)
- [21] D.H. Correa, J. Oliva and R. Troncoso, *JHEP* **08**, 081 (2008)
- [22] Gregory R. and Laflamme R., *Phys. Rev. Lett.* **70**, 2837 (1993)
- [23] Choptuik M.W. et al., *Phys. Rev. D*, **68**, 044001 (2003)
- [24] R. Emparan and H.S. Reall, *Living Rev. Relativity* **11**, 6 (2008)
- [25] G. Dotti and R.J. Gleiser, *Phys. Rev. D* **72**, 044018 (2005)
- [26] H. Kodama and A. Ishibashi, *Prog. Theor. Phys.* **111**, 29 (2004)
- [27] Tangherlini F.R., *Nuovo Cimento* **27**, 636 (1963)
- [28] G. Dotti and R.J. Gleiser, *Phys. Rev. D* **72**, 044018 (2005)
- [29] G. Dotti and R.J. Gleiser, *Phys. Rev. D* **72**, 124002 (2005)
- [30] Hawking S.W and Page D.N, *Comm. Math.Phys.* **87**, 577 (1983)
- [31] E. Berti, V. Cardoso and A.O. Starinets, *Class. Quantum Grav.* **26**, 163001 (2009)
- [32] H.P. Nollert, *Class. Quantum Grav.* **16**, R159 (2009)
- [33] K.D. Kokkotas and B. Schmidt, *Living Rev. Relativity* **2**, 2 (1999)
- [34] R.A. Konoplya and A. Zhidenko, *Rev. Mod. Phys.* **83**, 793 (2011)

-
- [35] R.A. Konoplya, *Phys. Rev. D* **66**, 044009 (2002)
- [36] H.T. Cho et al., *Advances in Mathematical Physics* Vol. **2012**, Article ID 281705.
- [37] G. T. Horowitz and V. E. Hubeny, *Phys. Rev. D* **62**, 024027 (2000)
- [38] J.D. Bekenstein, *Lett. Nuovo Cimento Soc. Ital. Fis.* **11**, 467 (1974)
- [39] S. Hod, *Phys. Rev. Lett.* **81**, 4293 (1998)
- [40] Lanczos C., *Z. Phys.* **73**, 147 (1932)
- [41] Lanczos C., *Annals Math.* **39**, 842 (1938)
- [42] O. Dreyer, *Phys. Rev. Lett.* **90**, 081301 (2003)
- [43] M. Maggiore, *Phys. Rev. Lett.* **100**, 141301 (2008)
- [44] S. Ryu and T. Takayanagi, *Phys. Rev. Lett.* **96**, 181602 (2006)
- [45] S. Ryu and T. Takayanagi, *JHEP* **07**, 62 (2007)
- [46] S. Ryu and T. Takayanagi and T. Nishioka, *J. Phys. A: Math. Theor.* **42**, 504008 (2009)
- [47] T. Takayanagi, *Class. Quantum Grav.* **29**, 153001 (2009)
- [48] P. Dey and S. Roy, *Phys. Rev. D* **87**, 066001 (2013)
- [49] S. Ryu and T. Takayanagi, *JHEP* **08**, 045 (2006)
- [50] J. Crisostomo, R. Troncoso and J. Zanelli, *Phys. Rev. D* **62**, 084013 (2000)

-
- [51] S. Musiri and G. Siopsis, *Phys. Lett. B* **576**, 309-313 (2003)
- [52] G. Kunstatter, *Phys. Rev. Lett.* **90**, 161301 (2003)
- [53] D.G. Boulware and S. Deser, *Phys. Rev. Lett.* **55**, 2656 (1985)
- [54] J. T. Wheeler, *Nucl. Phys. B* **268**, 737 (1986)
- [55] Pablo Gonzalez et al., *JHEP* **1008**, 050 (2010)
- [56] Lovelock, D., *J. Math. Phys.* **12**, 498 (1971)
- [57] B. Mashhoon, *Phys. Rev. D* **31**, 290 (1985)
- [58] B. Mashhoon and H.J. Blome, *Phys. Lett. A* **100**, 231 (1984)
- [59] B.F. Schutz and C.M. Will, *Astrophys. J. Lett.* **291**, L33 (1985)
- [60] S. Iyer and C.M. Will, *Phys. Rev. D* **35**, 3621 (1987)
- [61] E. Leaver, *Proc. R. Soc. London* **A402**, 285 (1985)
- [62] L. Motl and A. Neitzke, *Adv. Theor. Math. Phys.* **7**, 307-330 (2003)
- [63] V. Cardoso et al., *Phys. Rev. D* **79**, 064016 (2009)
- [64] V. Ferrari and B. Mashhoon, *Phys. Rev. D* **30**, 295 (1984)
- [65] S. A. Hartnoll, *Class. Quant. Grav.* **26**, 224002 (2009)
- [66] E. Berti and K. D. Kokkotas, *Phys. Rev. D* **71**, 124008 (2005)
- [67] A. Strominger and C. Vafa, *Phys. Lett. B* **379** 99–104 (1996)
- [68] S. D. Mathur, *Fortsch. Phys.* **53** 793–82 (2005)
- [69] S. D. Mathur, *Class. Quant. Grav.* **23** R115 (2006)

-
- [70] S. Chandrasekhar, *The Mathematical Theory of Black Holes* (1983)
- [71] R.A. Konoplya, *Phys. Rev. D* **68**, 024018 (2003)
- [72] <http://fma.if.usp.br/konoplya/>
- [73] Chen Ju-Hua and Wang Yong-Jiu, *Chin. Phys. B* Vol.**19**, No. 6, 060401 (2010)
- [74] S W Hawking, *Nature* **248**, 30 (1974)
- [75] S W Hawking, *Comm. Math. Phys.* **43**, 199 (1975); Erratum: *ibid.* **46**, 206 (1976)
- [76] S W Hawking, *Phys. Rev. D* **13**, 191 (1976)
- [77] S. W. Hawking, *Phys. Rev. Lett.* **26**, 1344 (1971)
- [78] J. D. Bekenstein, *Phys. Rev. D* **7**, 2333 (1973)
- [79] J. M. Bardeen, B. Carter and S. W. Hawking, *Commun. Math. Phys.* **31**, 161 (1973)
- [80] R. Penrose, *Riv. Nuovo Cimento* **1**, 252 (1969)
- [81] M. Cvetič and S. S. Gubser, *JHEP* **04**, 024 (1999)
- [82] C. V. Vishveshwara, *Nature* **227**, 936 (1970)
- [83] E. Sorkin, *Phys. Rev. Lett.* **93**, 031601 (2004)
- [84] Vitor Cardoso, José P. S. Lemos and Shijun Yoshida, *gr-qc/0309112v2*
- [85] R. A. Konoplya, *hep-th/0309030v4*

-
- [86] R. A. Konoplya, *gr-qc/0207028v3*
- [87] Xiangdong Zhang, *arXiv:1506.05739v2*
- [88] M. M. Caldarelli, G. Cognola and D. Klemm, *Class. Quant. Grav.* **17**, 399 (2000)
- [89] E. Witten, *Adv. Theor. Math. Phys.* **2**, 505 (1998)
- [90] A. Sahay, T. Sarkar and G. Sengupta, *JHEP* **1011**, 125 (2010)
- [91] R. Banerjee, S. K. Modak and S. Samanta, *Eur. Phys. J. C.* **70**, 317 (2010)
- [92] R. Banerjee, S. K. Modak and S. Samanta, *Phys. Rev. D* **84**, 064024 (2011)
- [93] Q. J. Cao, Y. X. Chen and K. N. Shao, *Phys. Rev. D* **83**, 064015 (2011)
- [94] R. Banerjee and D. Roychowdhury, *Phys. Rev. D* **85**, 044040 (2011)
- [95] R. Banerjee, S. Ghosh and D. Roychowdhury, *Phys. Lett. B* **696**, 156 (2011)
- [96] R. Banerjee and D. Roychowdhury, *JHEP* **11** 004 (2011)
- [97] R. Banerjee, S. K. Modak and D. Roychowdhury, *JHEP* **1210**, 125 (2012)
- [98] S. W. Wei and Y. X. Liu, *Europhys. Lett.* **99**, 20004 (2012).
- [99] B. R. Majhi and D. Roychowdhury, *Class. Quantum Grav.* **29**, 245012 (2012)

-
- [100] W. Kim and Y. Kim, *Phys. Lett. B* **718**, 687 (2012)
- [101] Y. D. Tsai, X. N. Wu and Y. Yang, *Phys. Rev. D* **85**, 044005 (2012)
- [102] F. Capela and G. Nardini, *Phys. Rev. D* **86**, 024030 (2012)
- [103] D. Kubiznak and R. B. Mann, *JHEP* **1207**, 033 (2012)
- [104] C. Niu, Y. Tian and X. N. Wu, *Phys. Rev. D* **85**, 024017 (2012)
- [105] A. Lala and D. Roychowdhury, *Phys. Rev. D* **86**, 084027 (2012)
- [106] A. Lala, *Critical phenomena in higher curvature charged AdS black holes*, [arXiv:1205.6121]
- [107] S. W. Wei and Y. X. Liu, *Phys. Rev. D* **87**, 044014 (2013)
- [108] M. Eune, W. Kim and S. H. Yi, *JHEP* **1303**, 020 (2013)
- [109] M. B. J. Poshteh, B. Mirza, Z. Sherkatghanad, *Phys. Rev. D* **88**, 024005 (2013)
- [110] J. X. Mo and W. B. Liu, *Phys. Lett. B* **727**, 336 (2013)
- [111] Rao C.R., *Bull. Calcutta Math. Soc.* **37**, 81 (1945)
- [112] J. L. Alvarez, H. Quevedo and A. Sanchez, *Phys. Rev. D* **77**, 084004 (2008)
- [113] Gibbs. J., *The Collected Works Vol. 1, Thermodynamics*, Yale University Press, 1948.
- [114] Hermann. R., *Geometry, Physics and Systems*, Marcel Dekker N. Y. (1973).
- [115] Mrugala. R., *Rep. Math. Phys.* **14**, 419 (1978)

-
- [116] Mrugala. R., *Rep. Math. Phys.* **21**, 197 (1985)
- [117] Weinhold. F., *J. Chem. Phys.* **63**, 2479, 2484, 2488, 2496 (1975); **65** (1976) 558.
- [118] Ruppeiner. G., *Phys. Rev. A.* **20**, 1608 (1979)
- [119] H. Quevedo and A. Sanchez, *JHEP.* **09**, 034 (2008)
- [120] H. Quevedo, *J. Math. Phys. (N.Y.)* **48**, 013506 (2007)
- [121] H. Quevedo, *Gen. Relativ. Gravit.* **40**, 971 (2008)
- [122] H. Quevedo, A. Sanchez et al., *Gen. Relativ. Gravit.* **43**, 1153 (2011)
- [123] H. Janyszek, R. Mrugala, *Rep. Math. Phys.* **27**, 145 (1989)
- [124] G. Ruppeiner, *arXiv:1309.0901*
- [125] H. Quevedo and A. Sanchez, *Phys. Rev. D* **79**, 087504 (2009)
- [126] H. Quevedo and A. Sanchez, *Phys. Rev. D* **79**, 024012 (2009)
- [127] J. Suresh et al., *JHEP* **01**, 019 (2015)
- [128] J. Suresh et al., *Eur. Phys. J. C* **74**, 2819 (2014)
- [129] R. Tharanath et al., *Gen. Rel. Grav.* **47**, 46 (2015)
- [130] R. Tharanath et al., *Gen. Rel. Grav.* **46** 1743 (2014)
- [131] A. Ashtekar et al., *Phys. Rev. Lett.* **80**, 904 (1998)
- [132] B. P. Abbot et al., *Phys. Rev. Lett.* **116**, 241103 (2016)
- [133] S.D.H. Hsu, *Phys. Lett. B* **664**, 67 (2007)

-
- [134] J. Bekenstein and V. F. Mukhanov, *Phys. Lett. B* **360**, 7 (1995)
- [135] J.D. Bekenstein, *arXiv:9710076[gr-qc]*
- [136] J.D. Bekenstein, *arXiv:9808028[gr-qc]*
- [137] S. Hod, *Phys. Rev. Lett.* **81**, 4293 (1998)
- [138] Hod S., *Gen. Rel. Grav.* **31**, 1639 (1999)
- [139] Setare M. R. and Vagenas E. C., *Mod. Phys. Lett. A.* **20**, 1923 (2005)
- [140] Setare M. R., *Class. Quant. Grav.* **21**, 1453 (2004)
- [141] Setare M. R., *Phys. Rev. D* **69**, 044016 (2004)
- [142] Setare M. R., *Gen. Rel. Grav.* **37**, 1411 (2005)
- [143] Medved A. J. M., *Class. Quant. Grav.* **25**, 205014 (2008)
- [144] Vagenas E. C., *JHEP* **0811**, 073 (2008)
- [145] D. Lovelock, *J. Math. Phys. (N.Y.)* **12** (1971) 498.
- [146] A. Bravetti et al., *Adv. High Energy Phys.* **2013**, 549808 (2013)
- [147] A. Bravetti et al., *Gen. Relativ. Gravit.* **45**, 1603 (2013)
- [148] B.R. Majhi and E.C. Vagenas, *Phys. Lett. B* **701**, 623 (2011)
- [149] Ivan Debono and George F. Smoot, *arXiv:1609.09781v1[gr-qc]*.
- [150] H. Kodama, *Prog. Theor. Phys.* **110**, 4, 701 (2003).